In: Landman, N.H., Plint, A.G. & Walaszczyk, I. (eds), 2017. Allostratigraphy and biostratigraphy of the Upper Cretaceous (Coniacian-Santonian) western Canada foreland basin. Bulletin of the American Museum of Natural History 414, 9-52.

Chapter 1

Integrated, High-Resolution Allostratigraphic, Biostratigraphic and Carbon-Isotope Correlation of Coniacian Strata (Upper Cretaceous), Western Alberta and Northern Montana

A. GUY PLINT,[1] ELIZABETH A. HOOPER,[1]
MERIEM D. GRIFI,[2] IRENEUSZ WALASZCZYK,[3] NEIL H. LANDMAN,[4]
DARREN R. GRÖCKE,[5] JOÃO P. TRABUCHO ALEXANDRE,[6]
AND IAN JARVIS[7]

ABSTRACT

Lower to upper Coniacian rocks in the foredeep of the Western Canada Foreland Basin are dominated by mudstone and subordinate sandstone and were deposited on a very low-gradient, storm-dominated marine ramp. The rocks are organized into several scales of upward-coarsening, upward-shoaling succession, bounded by marine flooding surfaces. Abundant, publicly available wireline log data permit flooding surfaces to be traced for hundreds of kilometers in subsurface. Flooding surfaces can be considered to approximate time surfaces that allow the subsidence history of the basin to be reconstructed. Particularly widely traceable flooding surfaces were chosen, on pragmatic grounds, as the boundaries of 24 informal allomembers, most of which can be mapped along the foredeep for >750 km. Allomembers can also be traced westward into the fold-and-thrust belt to outcrop in the Rocky Mountain Foothills. Some flooding surfaces are mantled with intra- or extrabasinal pebbles that imply a phase of shallowing and, potentially, subaerial emergence of part of the ramp.

The rocks yield a rich and well-preserved molluscan fauna dominated by inoceramid bivalves and scaphitid ammonites. Several major inoceramid speciation events are recognized. The lowest occurrence of *Cremnoceramus crassus crassus,* various species of *Volviceramus, Sphenoceramus subcardissoides,* and *S. pachti* all appear immediately above major flooding surfaces, suggesting that speciation,

[1] Department of Earth Sciences, The University of Western Ontario, London, Ontario, Canada.
[2] Husky Energy Inc., Calgary, Alberta, Canada.
[3] Faculty of Geology, University of Warsaw, Poland.
[4] Division of Paleontology, American Museum of Natural History.
[5] Department of Earth Sciences, Durham University, Durham, U.K.
[6] Department of Earth Sciences, Universiteit Utrecht, Utrecht, the Netherlands.
[7] Department of Geography and Geology, Kingston University London, Kingston upon Thames, U.K.

and dispersal of new inoceramid taxa were closely linked to episodes of relative sea-level rise. Thus, the boundaries of biozones can be shown to coincide with physical stratigraphic (flooding) surfaces. The generally rare species *Inoceramus gibbosus* is abundant in the upper part of the lower Coniacian; the preservation of this zonal form may be attributed to rapid subsidence of the foredeep that outpaced a major eustatic? sea-level fall that took place at the end of the early Coniacian and that is marked by a hiatus in most epicontinental basins. Regional mapping shows that allomembers, which have a near-tabular geometry, can be grouped into "tectono-stratigraphic units" that fill saucer-shaped, flexural depocenters. Individual depocenters appear to have been active for ca. 0.5 to 1.5 m.y., and successive depocenters are offset laterally, probably reflecting episodic shifts in the locus of active thickening in the Cordilleran orogenic wedge and related subsidence in the foreland basin. Preliminary carbon-isotope results from one section are tentatively correlated, using biostratigraphic tie-points, to the English Chalk reference curve: the Light Point, East Cliff, and White Fall carbon-isotope events (CIE) are recognized with some degree of confidence. The astronomically calibrated succession of CIE in the English Chalk suggests that the 24 mapped allomembers in Alberta each had an average duration of about 125,000 yr. Because allomembers can be traced for hundreds of km, an allogenic control, probably eustasy, appears to be the most likely genetic mechanism.

INTRODUCTION

The Western Canada Foreland Basin (WCFB) contains a preserved stratigraphic succession, over 5 km thick, that forms an expanded record of terrestrial and shallow-marine sedimentation through much of the Late Jurassic, Cretaceous, and Paleocene (Wright et al., 1994). Well-exposed sections in the Rocky Mountain Foothills, coupled with a public database of tens of thousands of wireline logs and thousands of cores permit reconstruction of basin-scale stratal geometry, facies relationships, and paleogeography in a high-resolution allostratigraphic framework (e.g., Plint et al., 1986; Bhattacharya and Walker, 1991a, 1991b; Plint, 2000; Varban and Plint, 2008a, 2008b; Roca et al., 2008). Allostratigraphic units are mappable bodies of rock defined by bounding discontinuities (NACSN, 2005: Article 58). In the succession studied here, marine flooding or transgressive surfaces form the mappable bounding surfaces of allomembers. Such surfaces typically have low diachroneity relative to the time represented by the rock units that they bound, and hence can be considered to approximate time planes (e.g., Cross and Lessenger, 1988). In consequence, the WCFB provides an unparalleled natural laboratory in which to assess the principal physical controls on sedimentation, namely: sediment supply, tectonism, and eustasy. The temporal framework provided by physical, marine flooding surfaces also makes it possible to determine the temporal and spatial distribution of evolving lineages of molluscs that provide the principal basis for biostratigraphic correlation. It is then possible to address the question: Are biotic speciation and extinction events consistently associated with physical stratigraphic surfaces, and the relative sea-level changes that those surfaces are considered to represent?

The principal purpose of this paper is to present a very detailed allostratigraphic framework, developed for Coniacian strata across the foredeep of the Western Canada Foreland Basin. That framework then constitutes a physical, and near-temporal matrix in which to plot the vertical and lateral distribution of molluscan fossils, principally inoceramid bivalves and scaphitid ammonites. Full taxonomic documentation of the inoceramid and ammonite faunas is provided in companion papers (Landman et al. and Walaszczyk et al., this issue). A secondary objective is to present preliminary carbon-isotope data from Coniacian strata in Alberta, and to compare those results with the reference curve from the UK Chalk succession (Jarvis et al., 2006), and with results from coeval rocks in Colorado (Joo and Sageman, 2014). An interpretation of relative sea-

level changes is given in the companion papers by Landman et al. and Walaszczyk et al. (this issue).

Tectonic and Paleogeographic Overview of the Basin

Subsidence of the Western Canada Foreland Basin was initiated in the Jurassic as the result of isostatic flexure of underlying cratonic lithosphere under the load of the tectonically thickened Cordilleran fold-and-thrust belt to the west (Price, 1994; Evenchick et al., 2007). The earliest preserved foreland strata were deposited from the Late Jurassic (Kimmeridgian) to Early Cretaceous (Valanginian), when sediment was supplied to the Canadian portion of the basin by both local rivers and a continent-scale, north-flowing drainage system with headwaters in the southwestern and possibly also the southeastern United States (Williams and Stelck, 1975; Wright et al., 1994; Raines et al., 2013). In the Berriasian to Barremian, diminished tectonic activity in the Rocky Mountain Cordillera, resulted in widespread erosion and isostatic uplift of Upper Jurassic to Lower Cretaceous sediments in the foredeep (Leckie and Cheel, 1997; Leier and Gehrels, 2011). Subsidence of the Western Canada Foreland Basin resumed in the Aptian, accompanied by gradual marine flooding by a southward-advancing arm of the Polar Ocean. One or more continent-scale, north- and west-flowing river systems delivered sediment to the basin from headwaters in the Canadian Shield, the Appalachians, and the Cordillera (Benyon et al., 2014; Blum and Pecha, 2014).

At about the Albian-Cenomanian boundary (about 100.5 Ma), a southward-encroaching embayment of the Polar Ocean (the Mowry Sea) merged with a northward-encroaching arm of the Gulf of Mexico to form the early Greenhorn Sea (Williams and Stelck, 1975). This seaway continued to widen through the late Cenomanian to a maximum extent in the early Turonian, before progressive eustatic sea-level fall caused the seaway to narrow to a minimum in the late Turonian and earliest Coniacian, as recorded by rocks of the Cardium Formation (e.g., Nielsen et al., 2008; Shank and Plint, 2013; Walaszczyk et al., 2014). Earliest Coniacian regressive sandstones in the upper part of the Cardium Formation were buried by marine mudstone of the early to middle Coniacian Muskiki Member of the Wapiabi Formation. Muskiki strata record the onset of the Niobrara Cycle (Kauffman, 1977), which is expressed as a major transgression that drove the shoreline so far to the west that no near-shore deposits are preserved in outcrop sections exposed in the Alberta or British Columbia (BC) foothills (Stott, 1963, 1967; fig. 1). In late Coniacian time, the broadly regressive, siltstone- and sandstone-dominated Marshybank Member was deposited along the western margin of the basin. The slightly younger Bad Heart Formation was deposited in the northeastern part of the basin, and is confined to the Peace River Plains (Stott, 1963, 1967; Plint et al., 1990; Donaldson et al, 1998). Late Coniacian regression was followed by major regional transgression in latest Coniacian and early Santonian time, leading to widespread deposition of marine mudstone across Alberta and BC; this transgression coincided with a period of renewed flexural subsidence of the foredeep of the foreland basin (Nielsen et al., 2008; Hu and Plint, 2009; Plint et al., 2012a).

PREVIOUS STRATIGRAPHIC STUDIES

Lithostratigraphy

The early history of stratigraphic investigation of Upper Cretaceous rocks in Alberta was thoroughly reviewed by Stott (1963, 1967). The present study is focused on Coniacian rocks that form part of the Wapiabi Formation, a unit that was originally recognized and named by Malloch (1911). The Wapiabi Formation comprises up to about 650 m of marine mudstone with minor intercalations of sandstone and siltstone. Stott (1956, 1963, 1967) showed that the Wapiabi Formation could consistently be divided into seven members, each characterized by a distinct suite of lithologies that could be traced along most of the Rocky Mountain Foot-


Polar Ocean
60°N
Alberta
British Columbia
Study area
200 km
CANADA
USA
Montana
Western Interior Seaway
Pacific Ocean
30°N
Gulf of Mexico
Middle Coniacian (Scaphites (S.) ventricosus) – 87.9 Ma
© Colorado Plateau Geosystems

hills from NE BC to the Montana border (figs. 2, 3; *fig. 3 inserted after p. 52*). The lowest unit, the Muskiki Member, rests disconformably on the underlying Cardium Formation and comprises primarily offshore marine mudstone.

The boundary between the Muskiki and overlying Marshybank Member is typically a rapidly gradational to sharp contact between mudstone and siltstone and overlying, intensely bioturbated siltstone and silty sandstone. Toward the north, particularly north of the Athabasca River, the siltstone-dominated Marshybank Member undergoes a lateral facies change to include clean, well-sorted sandstone as well as siltstone and minor mudstone. Even further to the NW, in BC, the Marshybank includes not only near-shore sandstone but also a unit of terrestrial deposits (Plint and Norris, 1991). Stott (1967) did not extend the term "Marshybank" to describe these northern, sandstone-rich rocks, but instead chose to assign them to the "Bad Heart" Formation, inferring that sandy rocks in the foothills correlated with the type Bad Heart Formation that is exposed about 150 km to the NE on the Smoky River in the Peace River Plains. In the latter area, the Bad Heart Formation comprises fine-grained sandstone and ooidal ironstone with minor dark silty claystone.

A change of lithostratigraphic terminology occurs at the Canada–U.S. border: rocks of the Cardium and Wapiabi formations in Alberta being broadly correlative with the Ferdig and Kevin members of the Marias River Formation in Montana (Cobban et al., 1976; Nielsen et al., 2003; figs. 2, 3; figs. 3–13 inserted after p. 52).

Biostratigraphic Studies

Stott (1963, 1967) summarized existing biostratigraphic information regarding the age of the Wapiabi Formation. Stott reported that the lowest part of the Muskiki Member contained *Scaphites* (*S.*) *preventricosus* Cobban and *Inoceramus deformis* Meek. Stott used the stratigraphical interpretation of Jeletzky (who followed the traditional German subdivision) and dated these two taxa to the late Turonian, although he (Stott, 1963) did note that Jeletzky (personal commun.) considered that they might be of earliest Coniacian age (as treated at that time in the U.S.; see e.g., Seitz, 1959). The higher part of the Muskiki contained *Scaphites* (*S.*) *ventricosus* Meek and Hayden and *Inoceramus involutus* Sowerby, indicative of a Coniacian age. Neither *I. involutus* nor *S.* (*S.*) *ventricosus* were found to range up into the Marshybank Member (Stott, 1963). The Marshybank Member contained *Scaphites* (*S.*) *depressus* Reeside, which Stott did not find below the base of the member. At the time of Stott's studies, *S.* (*S.*) *depressus* was considered by Jeletzky (see also discussion in Obradovich and Cobban, 1975) to indicate an early Santonian age, but that zone was later reassigned to the upper Coniacian (Kennedy and Cobban, 1991). Collom (2001) undertook a litho- and biostratigraphic study of the Wapiabi Formation and equivalent strata between Highwood River in the south and the lower Smoky River in the north. Collom's correlation of depositional cycles along the Foothills was, however, made without reference to subsurface data, and his stratigraphic sections contain insufficient detail to be related to our own observations. Moreover, Collom's inoceramid taxonomy, and consequently his stratigraphic interpretation, cannot be confirmed in most of the cases (see companion paper by Walaszczyk et al., this issue).

In Montana, Cobban et al. (1976) recognized ammonite and bivalve zones in the Fer-

FIG 1. Paleogeographic reconstruction of North America for the middle Coniacian (*Scaphites* (*S.*) *ventricosus* time). This map is representative of the paleogeography during deposition of the Muskiki Member of the Wapiabi Formation when the Coniacian transgression was at approximately its greatest extent. The study area in Alberta and Montana is indicated. (Map adapted from R. Blakey, http://cpgeosystems.com).

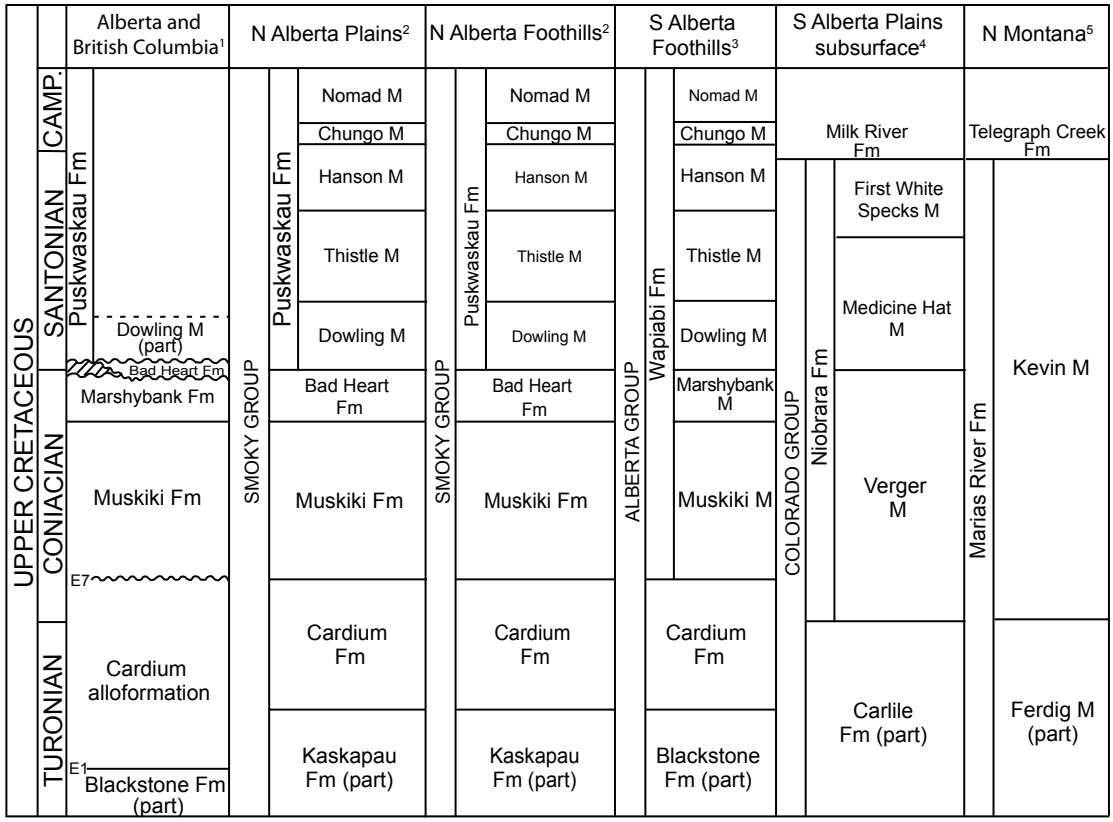

FIG. 2. Summary of stratigraphic schemes that have been applied to Upper Cretaceous strata in Alberta, British Columbia and northern Montana. The far left column shows the allostratigraphically defined limits of the Cardium alloformation, the base of which (surface E1) is placed below the lithostratigraphically defined position of Stott (1963, 1967).

dig and Kevin members of the Marias River Formation, allowing them to establish a broad correlation with the Cardium Formation and the Muskiki and Marshybank members of the Wapiabi Formation in Alberta. Cobban et al. (2005) made a detailed study of a thin (typically 10–20 cm) carbonate-cemented conglomerate bed (Bed 100 of the Kevin Member; Cobban et al., 1976) that, because it was so distinctive and widespread, was named by Cobban et al. (1959) the MacGowan Concretionary Bed. The bed contains small, well-rounded chert pebbles as well as reworked phosphate nodules and molluscan fossils. This bed lies at, or just above, the boundary between middle and upper Coniacian strata. A second bed of green-stained phosphate nodules, some of which are bivalve steinkerns, is located 3.5 m above the MacGowan Bed at the Type Section of the Kevin Member (Bed 108 of Cobban et al., 1976). Cobban et al. (2005) speculated that the MacGowan Bed in Montana might be correlative with the erosion surface documented beneath the Bad Heart Formation in Alberta, 850 km to the NW (Plint et al., 1990; Donaldson et al., 1998, 1999).

ALLOSTRATIGRAPHIC STUDIES

Previous Work

Regional allostratigraphic correlation of Coniacian rocks was initially conducted in northwestern Alberta and adjacent BC, where it was shown that upward-coarsening successions, bounded by marine flooding surfaces, could be traced for several hundred km in the subsurface, and also correlated into outcrop (Norris, 1989; Plint, 1990; Plint et al., 1990; Plint and Norris, 1991). These studies showed that the erosion surface that defined the *top* of the "Bad Heart" Formation in the foothills could be correlated with an erosion surface that defined the *base* of the type Bad Heart in the Peace River Plains. Plint et al. (1990) therefore proposed that Stott's term "Marshybank" be applied to *all* siltstone and sandstone facies overlying the Muskiki mudstones, throughout the foothills (fig. 2). The sandy and ooidal Bad Heart Formation was shown to be restricted to the plains, where it onlaps westward onto the top of the Marshybank Member and pinches out before reaching outcrop (Donaldson et al., 1998, 1999). Subsequent study of additional outcrop and surface sections in the Peace River Plains, coupled with dinoflagellate biostratigraphy, confirmed the existence and significance of the erosional contact between the Bad Heart Formation and the underlying Muskiki Formation, or older strata (Kafle et al., 2013).

Within the Muskiki Member, Plint (1990) traced two regional flooding surfaces, informally termed M1 and M2 (equivalent to surfaces CS4 and CS15 in the present study), and also divided the Marshybank Member into 12 informal "units, termed A through L, bounded by erosion surfaces. Simple upward-coarsening "parasequences" in the offshore part of the basin could be traced westward (landward) to areas where the rocks became sandier and commonly included clean, well-sorted, hummocky- and swaley-cross-stratified sandstone deposited in a shoreface environment (Plint, 1991; Plint and Norris, 1991). Where exposed in the Rocky Mountain Foothills, most shoreface sandstone bodies have a sharp, erosional basal contact that was interpreted as evidence for deposition during relative sea-level fall (Plint, 1991; Plint and Norris, 1991). Thus it could be shown that upward-shoaling "parasequences" deposited offshore, passed laterally landward into "sequences" that preserved evidence for both relative sea-level rise and fall. The sharp-based shoreface sandbodies in the Marshybank Member provided some of the initial stimulus to develop the concept of "forced regression" (Plint, 1991), and ultimately, contributed to the establishment of the falling-stage systems tract (Plint and Nummedal, 2000), which is now the widely accepted "fourth component" of the standard depositional sequence model (e.g., Catuneanu, 2006).

A reconnaissance study by Durbano (2009), extended allostratigraphic correlations southward, enabling Grifi (2012) to establish an allostratigraphic scheme for Coniacian rocks over 60,000 km^2 of southern Alberta, extending from Township 26 southward into the most northerly Montana Plains (fig. 3, *inserted after p. 52*). Grifi (2012) extended correlations from the subsurface of Alberta and Montana to outcrop sections, including the Type Section of the Kevin Member of the Marias River Formation, and to various sections in the Alberta Foothills. It was shown that depositional sequences in the lower (Coniacian) part of the Kevin Member in the Type Section near Kevin, MT, could be correlated, via wireline logs, to the Muskiki and Marshybank rocks in Canada (Grifi et al., 2013). Current investigation (Hooper, in prep.) has now linked the correlations of Plint (1990) and Grifi (2012) in the area between townships 26 and 44 (fig. 3).

Data and Methods

The results reported here are founded on a series of linked studies that, collectively, involved over 4800 wireline well logs, 74 outcrop sections, and 30 cores, spanning about 200,000 km^2 of the foredeep in Alberta and northern Montana (Norris, 1989; Plint, 1990; Plint and Norris, 1991; Donaldson, 1997; Donaldson et al., 1998, 1999; Durbano, 2009;

Grifi, 2012; Grifi et al., 2013; Hooper, Ph.D. in prep.; fig. 3, *after p. 52*). Allostratigraphic units were defined by marine flooding surfaces, recognizable in wireline logs by an abrupt increase in gamma-ray intensity and a decrease in resistivity, corresponding to an increase in clay content. These surfaces were traced and "looped" through grids of log cross sections to ensure that they were correlated consistently (figs. 4–13, *inserted after p. 52*). Outcrop sections in the foothills were palinspastically restored using balanced structural cross sections constructed by Rottenfusser et al. (2002) on the basis of outcrop mapping, drilling, and seismic data. On the base map (fig. 3), outcrop sections relevant to the present study are shown in their present and restored positions, and distances between wells and outcrop are noted on the cross sections (figs. 4–13, *after p. 52*).

Most major outcrop sections of Coniacian strata exposed in the Rocky Mountain Foothills were measured in detail, with particular attention paid to depositional cyclicity and bounding surfaces that were indicative of relative sea-level changes (appendix 1). A gamma-ray log was made for selected outcrop sections using an *Exploranium GR-130* portable gamma-ray spectrometer, with a sampling period of 30 seconds per site. Simultaneous collection of in situ molluscan macrofauna was conducted, with specimens located precisely in each measured section.

All fossil material collected during this investigation is archived at the Royal Tyrrell Museum of Palaeontology. Details of specimens and accession numbers are given in Walaszczyk et al. and Landman et al., in this issue.

Allostratigraphic Terminology

In order to make an allostratigraphic description of the Muskiki and Marshybank strata, it is necessary to give names to both the stratigraphic *surfaces* that bound rock units as well as to the *rock units* themselves. In the following discussion, the regionally mappable flooding surfaces within Coniacian rocks have been designated as CS1 (Coniacian surface 1) to CS23. The erosion surface separating the Cardium Formation from the overlying Muskiki Member is termed E7 following Plint et al. (1986), and the basal surface of Santonian strata is designated SS0 (Santonian surface 0). Allostratigraphically defined rock units are designated CA1 (Coniacian allomember 1) to CA24. Note that allomembers defined herein are considered to be informal stratigraphic units, designated by letters and numbers rather than formally defined names, and therefore are not capitalized in the text (NACSN, 2005).

Carbon-Isotope Analysis

Seven sections through Coniacian rocks (six outcrop, one core) were selected for carbon-isotopic analysis. Results of carbon-isotope analysis for the Cutpick Creek section (fig. 4) are reported here (appendix 2). At this site, 106 samples were collected at 1 m intervals from all lithologies except clean sandstone, in which the organic matter content was too low. Analyses were undertaken at the Stable Isotope Biogeochemistry Laboratory at the University of Durham. Rock samples were ground to a fine powder (ca. 10 μm) using a Retsch agate mortar grinder RM100. The bulk rock powders (ca. 5 mL) were decalcified overnight at room temperature (20° C) using a 3 M HCl solution in 50 mL centrifuge tubes. Insoluble residues were rinsed three or four times in deionized water, dried at 50° C, reground in an agate mortar, and stored in glass vials.

Organic carbon isotope ($\delta^{13}C_{org}$) measurements were performed on 2.5–3 mg splits of the insoluble residues using a Costech elemental analyser (ESC 4010) connected to a Thermo Scientific Delta V Advantage isotope ratio mass spectrometer via a Conflo III interface. Carbon isotope ratios are corrected for ^{17}O contribution and reported in standard delta (δ) notation in per mil (‰) relative to VPDB. Data accuracy was monitored through analyses of international and in-house standards calibrated against the international standards (viz., IAEA 600, USGS 24, and USGS 40). Analytical uncertainty for carbon isotope measurements was ±0.1‰ for replicate analyses of standards and <0.2‰ on replicate sample analyses.

Establishing Regional Allostratigraphic Correlations

A series of cross sections (figs. 4–13) that integrate wireline logs with outcrop sections, form the physical basis for the new allo- and biostratigraphic scheme presented here. To constrain the stratigraphic relationships between separate outcrop sections scattered along the Rocky Mountain Foothills, a summary, strike-oriented (NW–SE) well-log cross section was constructed (fig. 4), extending more than 750 km from Cutpick Creek, NW Alberta (in the vicinity of Grande Cache; Township 58, latitude 54° 5′ N), to Kevin, Montana (latitude 49° 45′ N; fig. 3). The correlations shown in the strike section are tightly constrained by a large grid of cross sections to the north and east, which are not shown on the base map (Plint, 1990; Grifi, 2012, Hooper, Ph.D. in prep.; fig. 3). Each principal section exposed in the Foothills between Cutpick Creek in the north, and Kevin in the south was correlated to this master cross section using wireline logs, some of which were from wells drilled in the deformed belt (figs. 3, 5–13).

Systematic tracing of marine flooding surfaces through the regional correlation grids of Plint, (1990), Grifi (2012) and Hooper (in prep.), showed that 24 flooding surfaces, designated CS1 to CS23 and SS0, were particularly robust, and could be traced through large parts, if not all of the study area (figs. 4–13).

The Character and Significance of Flooding Surfaces

Although each of the studied allomembers is typified by one or more, upward-coarsening successions (e.g., fig. 14), the nature of the flooding surface that bounds each allomember is variable. Four categories of surface are recognized: either the surface lacks a coarse-grained lag, or one of three types of granule to pebble lag is present. It is important to appreciate that these lags, which may be up to about 20 cm thick, can also be very discontinuous across a given exposure, to the extent that, on a lateral scale of a few meters, coarse grains may be *entirely absent* from some parts of the flooding surface (fig. 15). In some places, it is clear that lag deposits are confined to shallow erosional depressions on the flooding surface (fig. 16).

No coarse-grained lag: Flooding surfaces CS2, CS3, CS7, and CS9 have no coarse-grained lag and are characterized by an abrupt upward transition from coarser- to finer-grained sediment at which there is no evidence for concentration or winnowing of coarser grains, or formation of an irregular erosion surface. This type of flooding surface provides no evidence of relative sea-level fall and concomitant sea-floor erosion, and therefore is parsimoniously interpreted to record only relative sea-level rise and shoreline transgression, accompanied by a decrease in the volume and caliber of sediment supplied to the shelf.

Lag of intrabasinal clasts: Flooding surfaces CS6 and CS14 locally have a lag comprising intrabasinal phosphate and/or siderite pebbles that range in diameter up to about 100 mm. These clasts are indicative of some degree of erosion, probably to a depth of at least several dm, sufficient to expose early diagenetic nodules and to allow their concentration on the erosion surface. The presence of reworked intraclasts suggests that a phase of relative sea-level fall terminated deposition of the underlying allomember. The absence of extrabasinal pebbles suggests that erosion took place subaqueously, although subaerial emergence can not be ruled out. Subsequent relative sea-level rise reduced current energy at the bed, allowing the clasts to be buried in mud.

Lag of mixed extra- and intrabasinal clasts: In foothills exposures, flooding surfaces E7 and CS1, CS4, CS8, CS11, CS13 and CS15 to CS23 inclusive are, at least locally, mantled with a mixture of extrabasinal chert pebbles, typically 5–15 mm in diameter, and intrabasinal phosphate and siderite pebbles, typically 20 to 100 mm in diameter. Because of the asymmetry of wave-generated currents in shallow water, pebbles are not transported seaward across a marine shelf for

FIG. 14. A portion of the Muskiki Member exposed in Sheep River (fig. 11), illustrating typical sandier-upward successions (arrows) bounded by flooding surfaces. The regionally mappable surface CS3 is indicated.

more than a few hundred m to a few km from shore (e.g., Clifton, 2006), and it is not possible to concentrate chert pebbles by winnowing underlying sediment lacking such clasts. It is therefore concluded that the presence of chert pebbles on a flooding surface is an indication that the surface had previously been subaerially exposed, when extrabasinal pebbles were supplied by rivers flowing to a lowstand shoreline. This interpretation was initially advanced to explain the extensive mantles of chert pebbles on erosion surfaces in the Cardium Formation (e.g., Plint et al., 1986). Applying similar reasoning, it is inferred that at least the more westerly parts of the chert pebble-bearing surfaces in the Muskiki and Marshybank members experienced a phase of subaerial exposure.

Lag of mixed extra- and intrabasinal clasts in a matrix of ferruginous clay ooids: In the southern portion of the study area, flooding surface

FIG. 15. **A.** Overview of surface CS1 exposed at river level at the mouth of Oldfort Creek (fig. 10). At right, a coarse-grained wave ripple composed of granules and small pebbles of chert and quartz rests sharply on regional erosion surface CS1. Traced laterally over only 3 m, the coarse lag pinches out and surface CS1 is manifest simply as a sharp mud-on-mud contact; scale bar = 20 cm. **B.** Detail of the coarse-grained wave ripple.

CS23 is overlain by 0.1 to 1.2 m of ooidal ironstone, the base of which is sharp but typically intensely burrowed by a *Glossifungites* ichnofauna (fig. 17). Well-rounded chert pebbles, typically 5–15 mm in diameter, and somewhat larger phosphate pebbles are distributed throughout the ooidal ironstone, which lacks stratification and appears to be highly bioturbated. Ooidal ironstone is commonly interpreted to form under conditions of protracted clastic sediment starvation, accompanied by repeated winnowing and erosion of the sea floor in shallow water (e.g., Donaldson et al., 1999, and references therein). Regional correlation shows that the ooidal ironstone, which forms a patchy blanket across southern Alberta and northern Montana, is spatially coincident with a region of subtle stratal upwarp, across which Upper Coniacian strata are either very thin or absent (Grifi, 2012; figs. 4, 9–11). Stratigraphic relationships therefore suggest that, for much of late Coniacian time, the region blanketed by ooidal ironstone was either subaerially emergent, or so shallowly submerged that no clastic sediment could be accommodated, leading to the formation of a regional unconformity. Deposition of ooidal

FIG. 16. Intraclastic pebble lag resting on surface SS0 at Thistle Creek west (fig. 5). **A.** General view of siderite pebbles seen from above; scale bar in each image = 20 cm. **B.** Detail of panel A showing pitted, bioeroded surface of a siderite pebble. **C.** Side view of conglomerate showing clasts filling a shallow erosional trough (arrows).

ironstone above the unconformity is interpreted to have taken place in shallow water across a clastic-starved ramp during the early stage of relative sea-level rise in latest Coniacian time. Toward the northwest, the ooidal ironstone appears to be stratigraphically equivalent to up to 20 m of sandy siltstone that forms allomember CA24; this wedge-shaped allomember accumulated in an area of active flexural subsidence.

Use of Distinctive Flooding Surfaces to Establish Correlation to Outcrop

In order to establish, on a regional scale, the stratigraphic distribution of molluscan faunas collected at outcrop, it was necessary to trace flooding surfaces westward from the master strike line (fig. 4), via well logs, to studied outcrop sections in the Rocky Mountain fold-and-thrust belt. For most sections, correlation to subsurface was relatively straightforward, based on matching upward-coarsening depositional successions, a process greatly facilitated by the outcrop gamma-ray log that provided an objective measure of lithology. It is emphasized that the process of outcrop to subsurface correlation was based, as far as was possible, on matching the scale and lithological character of depositional successions, and certain thick bentonites seen at outcrop, with those represented in the nearest wireline well logs; wherever possible, the distribution of molluscan fauna was not used as a basis for correlation. This approach was intended to provide an independent check

on the relationship between depositional cyclicity and the stratigraphic distribution of molluscan fossils. A number of distinctive physical stratigraphic markers helped to constrain correlations between outcrop and well log, as discussed below.

E7 surface. The E7 surface separates the Cardium Formation from the overlying Muskiki Member, and constitutes a prominent and robust stratigraphic marker across the basin. In the vicinity of the foothills and in the adjacent subsurface, E7 has up to several tens of meters of erosional relief in the form of NW–SE elongate, NE-facing "steps" (e.g., Wadsworth and Walker, 1991). In consequence, the thickness of rock between E7 and overlying surfaces CS1 and CS2 can vary dramatically, reflecting the progressive onlap and burial of preexisting topography by lower Muskiki sediments. The E7 surface has a ubiquitous mantle of extrabasinal chert and quartz pebbles, typically a few cm to a few dm thick.

Surface CS1. Surface CS1 is a robust log marker that caps a distinct, upward-coarsening succession of mudstone, siltstone, and very fine-grained sandstone. In most outcrop sections, CS1 is mantled by a few mm to a few cm of anomalously coarse-grained sediment that may range from medium-grained sand to granules or small siliceous pebbles that may be molded into large-scale wave ripples (fig. 15). This thin but distinctive, coarser-grained lag forms a consistent stratigraphic marker. In some sites (e.g., Oldfort Creek, fig. 10), the granule lag on CS1 was discontinuous across an exposure tens of meters wide (fig. 15), raising the possibility that the apparent absence of the lag at some sites (e.g., Blackstone River, fig. 6, Highwood River and Sullivan Creek, fig. 12) may be attributed simply to limited lateral exposure.

Surface CS4. Over much of the study area, surface CS4 caps a prominent, sandier upward heterolithic succession, typically 10–20 m thick, comprising cm-scale interbeds of wave-rippled, very fine-grained sandstone and mudstone in which the bioturbation index (BI) is very low (fig. 18A). In the more westerly foothills exposures, such as Bighorn Dam, Bighorn River, Wapiabi Creek, and Sheep River (fig. 18B, C), CS4 is mantled by a mm to cm-scale lag of small phosphate and chert pebbles typically <5 mm in diameter, whereas in more eastern sections, this lag is absent.

Surface CS11. In the north, at Cutpick Creek (fig. 4) allomember CA11 is mantled by a few cm of chert and intraclastic pebbles dispersed through a sideritized mudstone matrix. Allomember CA11 has a distinctive log signature that can be traced southward in well logs (fig. 4). However, the upper surface, CS11 does not carry a pebble lag in the more southerly outcrop sections described here. Instead, at Chungo Creek, Bighorn Dam, Sullivan Creek, and Highwood River, CS11 is mantled by a sharp-based, cm-scale bed of clean, fine- to medium-grained sandstone that forms hummocky cross stratification (HCS) or combined-flow ripples, or fills gutter casts. This thin bed suggests some degree of storm-winnowing and erosion of the top of allomember CA11 that could be an expression of relative sea-level fall.

Surface CS14. Throughout the central foothills, between Thistle Creek (fig. 5) and Mill Creek (fig. 13), surface CS14 marks an abrupt facies boundary between underlying, cm-scale interstratified very fine-grained sandstone and mudstone, and overlying, intensely bioturbated siltstone and silty sandstone that characterizes the lithostratigraphic Marshybank Member (e.g., Stott, 1963; fig. 19A). In wireline logs, particularly toward the east, CS14 is manifest as a distinct "hot" spike on the gamma ray log, suggestive of an enrichment in clay and/or organic matter. Locally, as at Cardinal River (fig. 5), Burnt Timber Creek (fig. 9), and Sheep River (fig. 11), CS14 is mantled by a thin lag of siderite and phosphate pebbles. Toward the north, CS14 is truncated by CS15 (fig. 4).

Surface CS15. In the north at Cutpick Creek, CS15 is mantled by chert pebbles and lithic intraclasts. From north to south, CS15 progressively truncates allomembers CA11, 12, 13, 14, and 15 (fig. 4). Surface CS15 persists southward


A
Top
1.2 m
Ooidal ironstone
Surface CS23
Surface CS15 with phosphate & siderite pebbles
Surface CS14
B
C
Top
CS23
Thalassinoides

as a distinctive flooding surface until Township 36, where it is truncated by surface CS23. Traced westward, CS15 is a subtle flooding surface, locally mantled with chert and/or intraclastic pebbles, seen at Bighorn Dam and Bighorn River (fig. 7), Burnt Timber Creek (fig. 9), and Sullivan Creek (fig. 12).

Surface CS16. This surface caps a very widespread sandier-upward succession that, in the north, includes dm-scale sandstone beds with HCS, (e.g., Cutpick Creek, fig. 4). Within allomember CA16, stratified sandstone in the north grades laterally into highly bioturbated silty sandstone toward the south (e.g., figs. 5, 6, 7). Surface CS16 is mantled in the north by chert pebbles whereas to the south, pebbles are absent and the surface may be marked by a subtle flooding surface, or simply a band of large siderite nodules.

Surfaces CS17 to *CS22*. Surfaces CS17 to 22 are either mantled with a veneer of chert pebbles, or have an irregular, eroded upper surface and/or deep burrows, including *Thalassinoides*, suggestive of a firm-ground and early lithification. This suite of surfaces is here represented only at Cutpick Creek (fig. 4), but most of these surfaces have been traced for at least 150 km further to the NW of the present study area (Plint, 1990; Plint and Norris, 1991).

Surface CS23. An overall upward-coarsening succession is evident in the lithostratigraphic Marshybank Member (i.e., those rocks above CS14). The upper boundary of that regressive succession (i.e., the maximum regressive surface) is surface CS23 (fig. 20). This is a regional-scale surface that has been traced for 150 km to the north of the present study area (Plint, 1990), and for at least 300 km into Montana to the south of the study area (e.g., Cobban at al., 2005), for a minimum N–S extent of at least 1200 km (fig. 21). Surface CS23 is typically mantled by a lag of chert pebbles and/or intraclasts (phosphate, siderite) that form a layer that may range from a layer only one clast thick to a layer several dm (and exceptionally a few m) thick. South of about Township 26, and extending at least 170 km east to Range 13 W4, CS23 is overlain by 0.1 to 1.2 m of ooidal ironstone containing scattered small chert and phosphate pebbles, and typically pervasively cemented by siderite (Grifi, 2012; fig. 17). The basal surface of the ooidal ironstone is sharp, erosive, and typically highly burrowed (fig. 17). This pebbly ooidal ironstone is correlative with the MacGowan Concretionary Bed mapped over a large part of Montana by Cobban et al. (2005; fig. 4).

Surface SS0. Above CS23, bioturbated silty sandstone and siltstone form allomember CA24, which is an eastward-thinning unit up to about 20 m thick (e.g., fig. 8). CA24 comprises an overall upward-fining stack of meter-scale, upward-coarsening successions bounded by flooding surfaces that commonly are mantled by a mixture of chert, siderite and phosphate pebbles (e.g., fig. 16). Successive upward-coarsening successions show a gradual upward decrease in BI, with progressively better preservation of cm-scale primary stratification. The top of this relatively coarse-grained package is marked by a sharp or abruptly gradational (few cm) transition, at surface SS0, into dark grey, thinly bedded mudstone with a BI of 0–1, characterized by a much higher radioactivity than the underlying

FIG. 17. **A.** Ooidal ironstone containing small chert pebbles overlying a heavily bioeroded surface near the top of the Coniacian succession on Sullivan Creek (fig. 12). The base of the ironstone is flooding surface CS23. Flooding surface CS15 is mantled with cm scale rounded siderite and phosphate pebbles and surface CS14 marks the boundary between underlying, well-stratified sandstone and mudstone and overlying, highly bioturbated sandy siltstone. **B.** Detail of bioerosion on the base of the ooidal ironstone shown in (A). Arrows indicate cm scale *Thalassinoides*, whereas larger irregular erosional structures may also be attributed to *Thalassinoides*, but may be the result of burrowing by larger arthropods and are perhaps comparable to the "subway tunnels" described from the Cardium Formation (Pemberton et al., 1984); scale bar = 20 cm. **C.** Detail of the ooidal ironstone above surface CS23 at Mill Creek (fig. 13). A dense network of large *Thalassinoides* (arrows) penetrate up to 30 cm into the underlying sandy siltstone; hammer is 28 cm long.

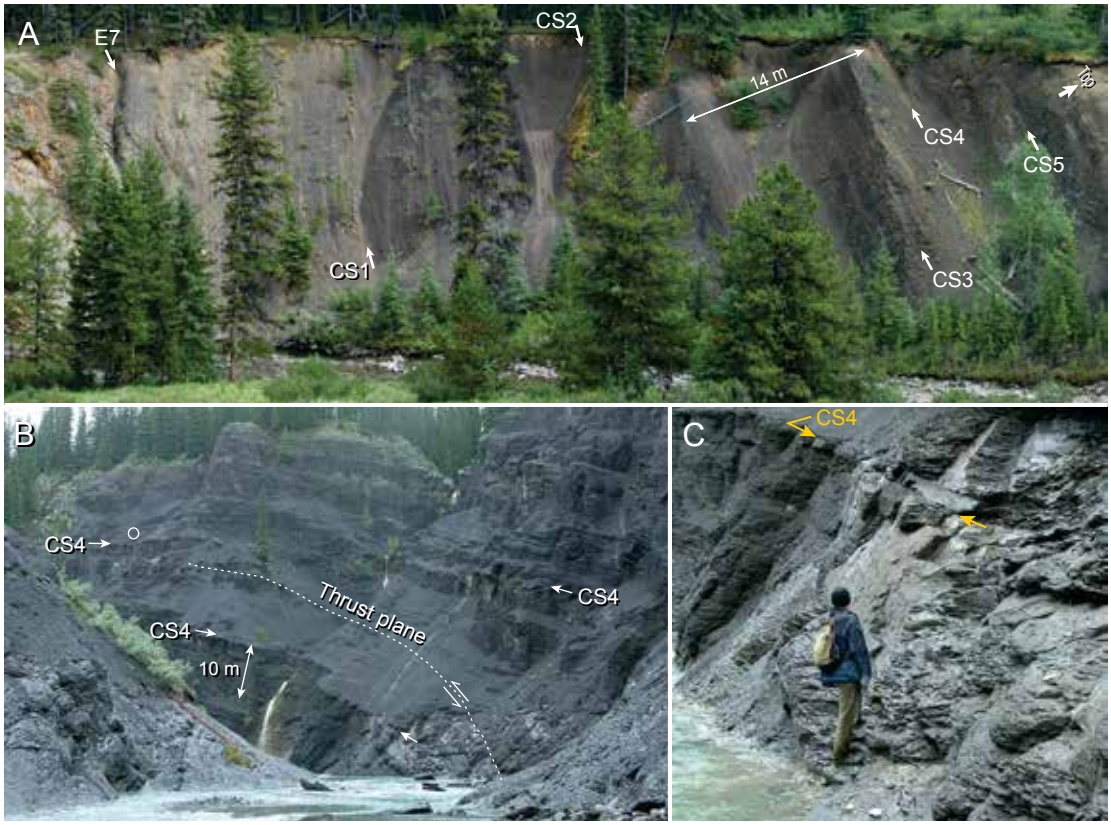

FIG. 18. **A.** Overview of the lower part of the Coniacian succession at Burnt Timber Creek (fig. 9) illustrating depositional cyclicity and bounding surfaces E7 and CS1 to CS5. Note the prominent sandier-upward succession culminating in surface CS4. **B.** Overview of part of the Sheep River canyon (fig. 11). The CS4 surface caps an upward-coarsening package that, in this view, is repeated by a thrust fault; Walaszczyk (circled) provides an indication of scale. **C.** Detailed view of the subtle, but sharp CS4 surface that is mantled with a few mm of chert and phosphate pebbles and granules and separates bioturbated siltstone and very fine-grained sandstone below from silty clay above.

rock (fig. 19B). SS0 is particularly prominent in the western part of the study area where the contrast between under- and overlying lithologies is greatest; SS0 gradually becomes more subtle toward the east as allomember CA24 thins. Toward the north, SS0 gradually onlaps onto surface CS23 such that the two surfaces are indistinguishable at the scale of well logs (fig. 4). Where exposed at Cutpick Creek, CS23 lies at the base of a 1 m thick conglomerate capping the Marshybank Member, and SS0 may lie at the same surface, or possibly may be unrecognizable within, or at the top of the conglomerate.

Continuity of Bounding Surfaces

Figures 4 to13 show that most of the flooding surfaces that bound allomembers can be traced as nearly parallel surfaces for at least 750 km along the strike of the proximal foredeep, and for many tens of km westward to outcrop. Locally, however, some allomembers do lap out. Allomembers CA1 and CA2 onlap locally against erosional topography on the underlying E7 surface (e.g., fig. 4 between wells 3-16-53-25W5 and 10-30-54-25W5). Allomembers CA3 to CA14 form a near-tabular set of strata, traceable throughout most of the strike section. However,

allomembers CA5 and CA9 lap out northward whereas CA6 and CA8 lap out southward (fig. 4). Allomembers CA16 to CA23 are confined to a northern depocenter (fig. 4), and extend beyond the northern limit of the present study area. To the east of the proximal foredeep, a number of disconformities have been recognized, across which various allomembers lap out, or are truncated (Hooper and Plint, 2016; Hooper, Ph.D. in prep.). These stratal terminations take place across narrow linear regions that might reflect differential subsidence and uplift across underlying structures (cf. Grifi et al., 2013); discussion of this aspect of the stratigraphy is beyond the scope of the present study.

SEDIMENTOLOGY

The focus of this paper is on regional stratigraphy and, in consequence, only a brief account of the principal sedimentary facies is given here. The Muskiki Member is dominated by mudstone with a variable proportion of interstratified fine- to very fine-grained sandstone, whereas the Marshybank Member includes both bioturbated sandy siltstone and various types of clean, well-sorted sandstone. Five facies are distinguished here.

Stratified silty mudstone typically has a low BI (0–2) and consists of mudstone interstratified with mm-scale, sharp-based beds of coarse siltstone that may have planar or wave-rippled upper surfaces. The rock may have a rusty weathering appearance, and siderite nodules vary from absent to common (fig. 22A, B). Silt and clay are interpreted to have been transported seaward, primarily by storm-generated combined flows (cf. Plint et al., 2012b; Buckley et al., 2016). A low level of bioturbation indicates a sparse metazoan infauna, suggestive of stressed conditions, probably attributable to a low dissolved oxygen content (i.e., 2–5 mg/L^{-1}) in the bottom water (cf. Dashtgard et al., 2015; Dashtgard and MacEachern, 2016). Rusty weathering is an indication of abundant disseminated pyrite. Siderite nodules are a relatively early diagenetic mineral, precipitated from pore water with a high bicarbonate (derived from organic matter), and low dissolved sulfide content, the latter having been removed by prior pyrite formation (McKay et al., 1995). This facies is interpreted to represent a relatively distal (order of 100 km or more) offshore environment, above storm wavebase for mud (?50–70 m water depth, cf. Plint et al., 2012b; Plint, 2014).

Bioturbated silty mudstone typically has a faintly stratified to rubbly appearance at outcrop as a result of intense bioturbation (BI 4–6; fig. 22C). Siderite nodules are common in this facies and may be scattered, or concentrated in bands. A high degree of bioturbation indicates a thriving metazoan infauna, suggesting a bottom water dissolved oxygen level of >5 mg/L^{-1} (Dashtgard et al., 2015). Common siderite suggests that a higher level of oxygen in the pore water inhibited pyrite formation, allowing more iron to be available for siderite precipitation, which took place in the methanogenic zone, some distance below the sea floor (e.g., McKay et al., 1995). Sediment transport was primarily by storms and deposition took place closer to shore, and in somewhat shallower water than the stratified silty mudstone facies. The bottom water contained a higher dissolved oxygen content, promoting colonization by a benthic metazoan fauna.

Interstratified mudstone and very fine-grained sandstone is bedded on a cm scale (fig. 22A). Sandstone beds are always sharp-based, commonly with wave- or combined-flow ripples. The facies may have a red, rusty-weathering appearance, has a low BI (0–1) and generally lacks siderite nodules. The rusty-weathering appearance reflects abundant early diagenetic pyrite that formed in anaerobic pore fluids at a very shallow burial depth (McKay et al., 1995). Physical sedimentary structures indicate deposition from storm-generated combined flows above wavebase for very fine sand (?30–40 m). However, the low intensity of macroscopic bioturbation suggests that the bottom water had a low (i.e., 2–5 mg/L^{-1}) dissolved oxygen content that suppressed colonization by benthic macrofauna, resulting in well-preserved stratification.


A
Top
CS14
6 m
CS15
B
Top
151.5 m
141 m
Surface SS0
137.5 m
133 m

Bioturbated sandy siltstone to silty sandstone characterizes the more southern portion of the Marshybank Member (e.g., at Cardinal River, Bighorn Dam, Ram River, Cripple Creek; figs. 5, 7, 8). This facies appears abruptly above surface CS14 and persists to surface SS0 (fig. 19A). Although cm-scale beds of very fine-grained sandstone are discernable at intervals, most of the rock lacks stratification as a consequence of intense bioturbation (BI 5-6) by infauna of the *Cruziana* ichnofacies. Rounded nodules of siderite, typically 10–30 cm in diameter, are commonly arranged in bands throughout the facies. In far western exposures, such as Bighorn River, dm-scale, sharp-based, moderately bioturbated, very fine-grained sandstone beds are preserved (fig. 20B). Overall, this facies is interpreted to represent an inner shelf to lower shoreface environment in perhaps 10–30 m of water. Preserved, sharp-based sandstone beds suggest deposition from storms. However, pervasive bioturbation has destroyed most primary sedimentary structures, indicating that the sediment hosted a thriving metazoan infauna, supported by well-oxygenated bottom water and an abundant supply of organic matter (e.g., MacEachern et al., 2010; Dashtgard et al., 2015). The overall upward-coarsening succession between surfaces CS14 and CS23 suggests long-term shoreline progradation, upon which numerous minor, higher-frequency transgressive-regressive events were superimposed. The great lateral extent (>>100 km) of these minor successions suggests an allogenic (sea-level) rather than autogenic control. Depositional successions from CS23 upsection to SS0 are also composed of this facies, but are organized in an overall back-stepping, upward-fining pattern suggestive of long-term shoreline transgression, culminating in dark stratified mudstone above SS0 (fig. 19B).

Well-sorted sandstone with minor siltstone is confined to the northern portion of the Marshybank Member. The basic sedimentary motif comprises sandier-upward successions of siltstone and sandstone (fig. 23). Siltstones are commonly moderately to highly bioturbated (BI 3–6) whereas sandstones are well-sorted, well-stratified and generally weakly bioturbated. Sharp-based, cm- to dm-scale beds of very fine-grained sandstone commonly preserve wave ripples and hummocky cross stratification with a variable overprint of bioturbation. Meter-scale, sharp-based, fine-grained sandstone bodies show swaley cross stratification or planar lamination (fig. 23). Sandstone in this facies provides good evidence for deposition under the influence of storm waves in an inner shelf to shoreface setting (e.g., Cheel and Leckie, 1993; Plint, 2010). Swaley cross-stratified sandstone bodies are sharp-based, typically underlain by large gutter casts, and are assigned to the falling-stage systems tract, interpreted to have been deposited during relative sea-level fall (Plint and Nummedal, 2000). The stacked, upward-shoaling, shelf to shoreface successions can be mapped for 200 to 300 km along strike, suggesting that they record an allogenic, sea-level control, rather than a more localized autogenic effect such as delta-lobe switching.

Principal Molluscan Zones

Although physical allostratigraphic correlation provides a good basis for understanding regional stratigraphy, confidence in correlation is greatly strengthened by integration of key ele-

FIG. 19. **A.** Overview of the upper part of the Coniacian succession at Cardinal River, showing the sharp boundary at surface CS14 that separates well-stratified mudstone and sandstone below from intensely bioturbated silty sandstone above. **B.** Overview of the upper part of the Coniacian succession at Ram River, showing the transition from intensely bioturbated silty sandstone below 137.5 m level, into bioturbated siltstone up to 141 m, above which siltstone gradually becomes darker and contains more inter-stratified very fine-grained sandstone up to surface SS0, above which the first Santonian fauna is found.

FIG. 20. **A.** The upper part of the Marshybank Member at the Bighorn Dam section (fig. 7). Surface CS23, which is mantled with chert and siderite pebbles, marks a maximum regressive surface and is overlain by four subtle upward-coarsening successions culminating in surface SS0. **B.** Upper part of the Marshybank Member exposed on the Bighorn River (fig. 7) showing bioturbated sandy siltstone grading up into weakly stratified silty sandstone, the top of which is marked by surface CS23.

ments of the molluscan fauna. Five key biostratigraphic events have been identified based on inoceramids (fig. 24; see Walaszczyk et al., this issue, for detailed discussion):

1. *Cremnoceramus crassus crassus* appears immediately above the E7 surface, as documented by Walaszczyk et al. (2014). This fauna persists up to surface CS4.
2. *Inoceramus gibbosus* fauna is present only in allomembers CA2–CA4 and is not found above surface CS4. This fauna characterizes the uppermost zone of the lower Coniacian.
3. *Volviceramus koeneni*, in association with *V. undabundus, V. exogyroides,* and *V. cardinalensis*, appears immediately above surface CS4, which marks the base of the middle Coniacian (see also Walaszczyk and Cobban, 2006). *V. involutus* appears slightly higher, above surface CS7.
4. *Sphenoceramus subcardissoides* appears in the upper part of allomember CA15, which is the basal unit of the upper Coniacian, defined by the first occurrence of *Scaphites* (*S.*) *depressus*.
5. *Sphenoceramus pachti* coappears with *Clioscaphites saxitonianus* immediately above surface SS0, and both mark the base of the Santonian.

Four key biostratigraphic events have also been identified based on scaphitid ammonites (Landman et al., this issue):

1. The lowest occurrence of *Scaphites* (*S.*) *preventricosus* is just above erosional surface E5.5 in the Cardium alloformation, which marks the beginning of a major transgression, just below the base of the lower Coniacian (Walaszczyk et al., 2014).
2. The lowest occurrence of *S.* (*S.*) *ventricosus* is immediately above surface CS2 in allomember CA3, just below an interpreted highstand and prior to major regression that culminates at surface CS4 that marks the lower to middle Coniacian boundary.
3. The lowest occurrence of *S.* (*S.*) *depressus* is in allomember CA15, immediately above surface CS14 in an overall regressive succession that marks the base of the upper Coniacian.
4. The lowest occurrence of *Clioscaphites saxitonianus* is at the base of the Santonian (surface SS0), coinciding with a major transgression and a marked change in facies to deeper-water, more offshore mudstone.

Carbon-Isotope Stratigraphy

Regional stratigraphic correlation (fig. 4) shows that the Cutpick Creek section contains six disconformities at surfaces E7, CS4, CS8, CS11, CS15, and CS23. In representing the carbon-isotope stratigraphy for this section, it is necessary to accommodate these hiatuses. The stratigraphic log, as well as the corresponding carbon-isotope curve, is therefore presented in an "expanded" form to include gaps that are approximately proportional to the thickness of the missing parts of the section (fig. 25). Tie-points between Alberta and the UK Chalk succession (Jarvis et al., 2006), were established on the basis of: (1) The lowest occurrence of *Cremnoceramus crassus crassus* immediately above the E7 surface and (2) The lowest occurrence of *Volviceramus koeneni* immediately above surface CS4. The lowest occurrence of *Clioscaphites saxitonianus* was inferred, based on correlations in figures 4–13, to be at or immediately above surface SS0. Unfortunately, neither scaphitid ammonites, nor *Sphenoceramus subcardissoides* or *S. pachti* are present in the UK Chalk succession and hence can not be used as biostratigraphic tie points.

The carbon-isotopic events recorded at Cutpick Creek are tentatively correlated to the English Chalk Reference curve (fig. 25). Greater confidence is placed in the correlation of the lower and lower-middle Coniacian strata where biostratigraphic control is good. The Light Point, East Cliff, and White Fall carbon-isotope events (CIE) appear to be recognizable with some degree of confidence. The carbon-isotope record at Cutpick Creek is also

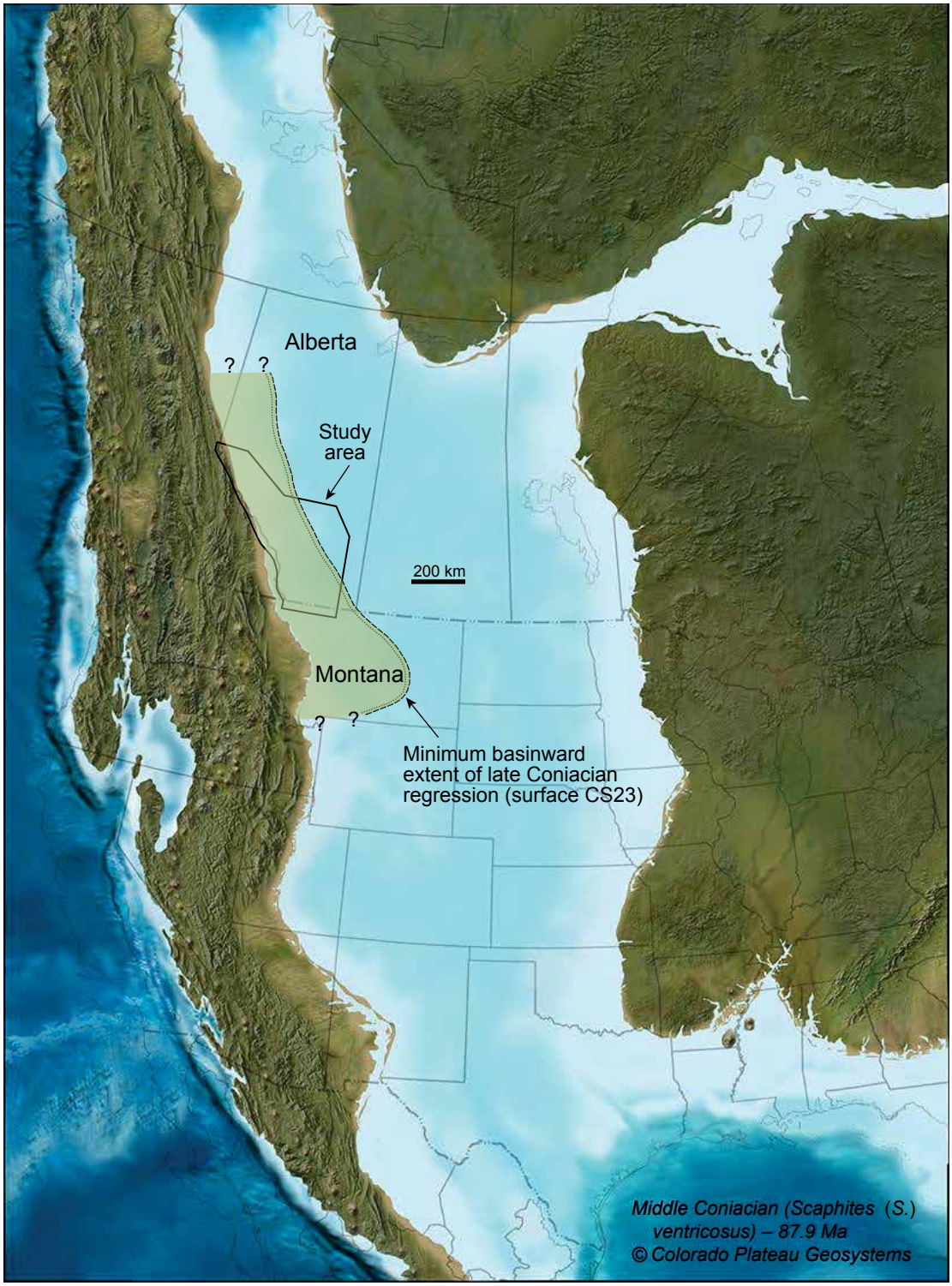
Alberta
? ?
Study
area
200 km
Montana
? ?
Minimum basinward
extent of late Coniacian
regression (surface CS23)
Middle Coniacian (Scaphites (S.)
ventricosus) – 87.9 Ma
© Colorado Plateau Geosystems

tentatively correlated with the Coniacian record from hemipelagic sediments sampled in the USGS Portland core in central Colorado (Joo and Sageman, 2014). Biostratigraphic control is provided by the lowest occurrences of *Volviceramus* and *Scaphites* (*S.*) *depressus*, allowing tentative correlation of the Light Point, East Cliff, and White Fall CIE.

Although a carbon-isotope curve was published for the upper Albian to Santonian succession in a core sampled at Cold Lake in eastern Alberta (Schröder-Adams et al., 2012), the location of that core, on the crest of the forebulge, has resulted in a very fragmentary stratigraphic record. The Lower Coniacian is not represented and the middle and upper Coniacian isotopic record has neither sufficient character nor biostratigraphic control to establish a correlation with the Cutpick Creek section.

GEOCHRONOLOGY

Nielsen et al. (2003, citing Obradovich, personal commun., 2000) reported argon-argon ages of 89.4± 0.31 and 89.19±0.51 Ma for two bentonites located, respectively, 1.8 and 2.6 m above the E7 surface in well 13-20-17-7W4. Allostratigraphic correlation (Grifi, 2012; Grifi et al., 2013) showed that the dated bentonites were located near the base of the Muskiki Member, between surfaces CS1 and CS2 of the present study (i.e., within allomember CA2). On the basis of these dated bentonites, Grifi et al. (2013) inferred an age of about 89.5 Ma for the E7 unconformity. The succession of CIE in the English Chalk (Jarvis et al., 2006), calibrated to an astronomical time scale (Laurin et al., 2015; fig. 25), allows the Coniacian succession in Alberta to be calibrated in terms of absolute age. Figure 25 indicates that the lowest occurrence of *C. crassus crassus,* at the E7 surface, is close to 89.51 Ma, suggesting that the bentonite ages reported in Nielsen et al. (2003) are consistent, within error, with the astronomically calculated ages for allomember CA2. The calibrated Chalk reference curve indicates that the base of the middle Coniacian (lowest occurrence of *Volviceramus*) is at about 88.99 Ma, implying that Muskiki allomembers CA1–CA4 collectively span just over 500,000 yr. The Coniacian–Santonian boundary is placed at 86.49±0.44 Ma by Sageman et al. (2014; fig. 25), implying that, collectively, the middle and upper Coniacian part of the Alberta succession (surfaces CA4–SS0) spans 2.5 m.y.

DISCUSSION

Tectonic Control on Deposition

Grifi et al. (2013) showed that, in southern Alberta, Coniacian rocks could be grouped into three distinct packages that had been deposited in three discrete depocenters. Allomember CA1 (equivalent to rocks between surfaces E7 and ME1 of Grifi et al., 2013) occupies an arcuate, westward-thickening basin centered at approximately Township 25, whereas allomembers CA2–CA10 (equivalent to rocks between surfaces ME1 and ME7 of Grifi et al., 2013) collectively occupy a SW-thickening basin with a center located south of the Alberta–Montana border. The abrupt alongstrike shift in the locus of flexural subsidence was attributed to a corresponding shift in the region of active tectonic thickening in the adjacent orogenic wedge. Allomembers CA12–CA15 (equivalent to rocks between surfaces ME7 and DE1 of Grifi et al., 2013) form a thin tabular sheet over the present study area, but thicken markedly to the east where they fill an elongate trough interpreted to have subsided as result of forced folding above an actively extending normal fault in the Precambrian basement (Grifi et al., 2013).

The patterns of subsidence recognized by Grifi et al. (2013) in the south can be traced northward through the present study area. The larger perspective afforded by the present study, coupled with geochronological control (figs. 25, 26), shows that lower Coniacian rocks (allomembers CA1–CA4) occupy

FIG. 21. Paleogeographic map showing the minimum extent of the erosion surface CS23 that forms the maximum regressive surface in the Upper Coniacian succession, and which is overlain by chert pebbles in west-central Alberta and BC, and by ooidal ironstone in southern Alberta and Montana. Chert pebbles provide definite evidence of subaerial emergence. Compiled from present study, Donaldson et al. (1998) and Cobban et al. (2005).

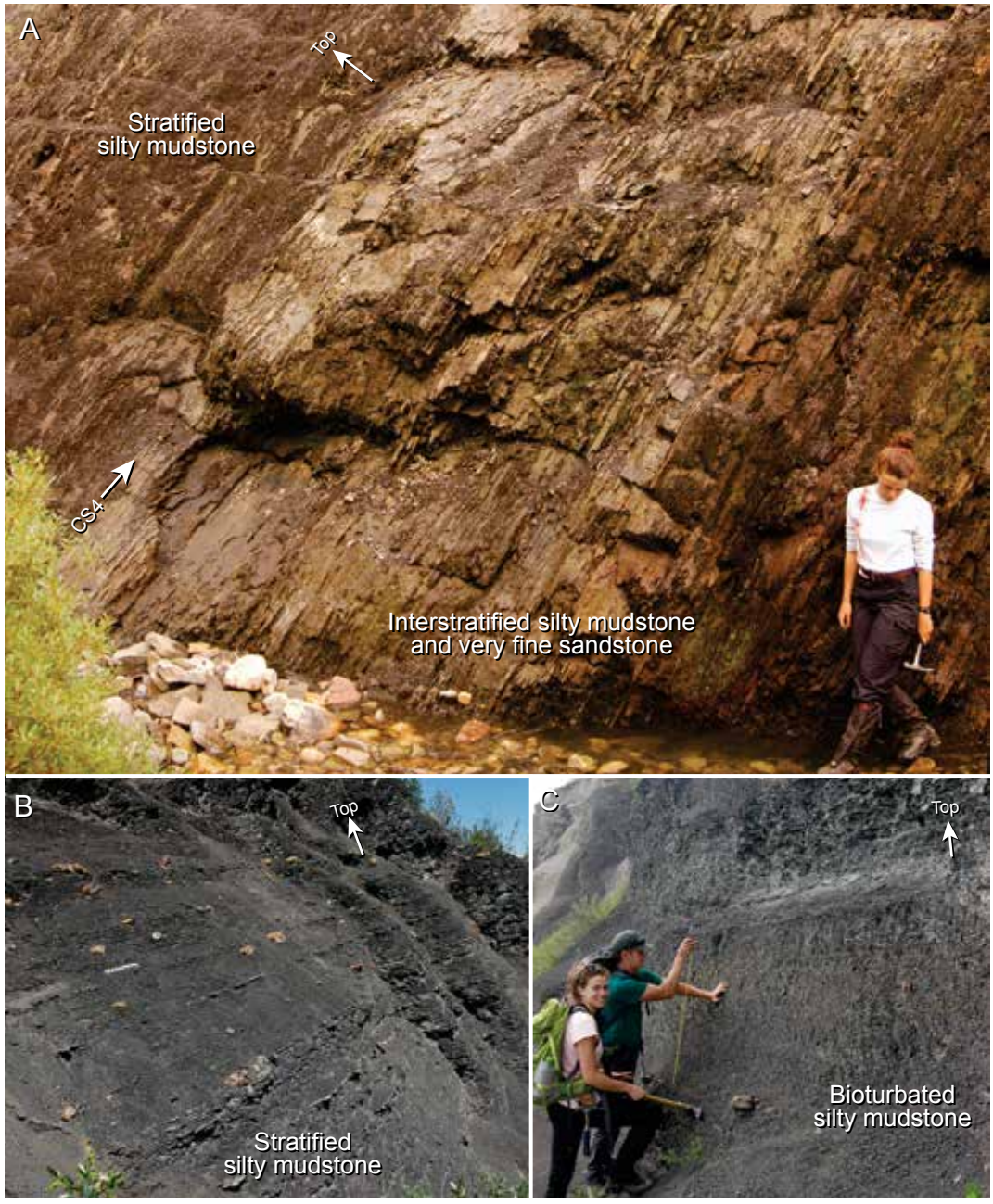

FIG. 22. Offshore facies typical of the Muskiki Member. **A.** Weakly bioturbated (BI 0-1) cm-scale beds of very fine-grained sandstone interstratified with mudstone forming an upward-coarsening succession culminating at flooding surface CS4. The rusty-weathering colour is typical of this facies and is due to abundant disseminated pyrite. Overlying rock comprises weakly bioturbated mudstone with mm-scale siltstone interbeds. Example: "Brown Creek" section (fig. 6, 11–19 m). **B.** Stratified mudstone (BI 1-2) with mm-scale coarse siltstone interbeds and abundant, dispersed siderite nodules; scale bar = 20 cm. Example: Oldfort Creek (fig. 10, 42–46 m). **C.** Heavily bioturbated (BI 4-5) sandy siltstone with dispersed siderite nodules. Example: Oldfort Creek (fig. 10, 49–52 m).

FIG. 23. Near-shore, sandstone-rich facies in the Marshybank Member in Cutpick Creek (fig. 4, 90–120 m). Bounding surfaces CS18 to CS23 and allomembers CA18 to CA23 are indicated. The upper part of CA18 contains fine-grained sandstone with hummocky cross stratification and the lower part of CA19 contains meter-scale, sandstone-filled gutter casts. The upper part of CA19 and most of CA20 consists of well-sorted, swaley cross-stratified, fine-grained sandstone. Centimeter-scale fine sandstone beds in CA21 to CA23 are planar laminated and wave rippled.

FIG. 24. Summary chart showing the stratigraphic distribution of fossils within the 24 allomembers mapped through the study area.

Bounding surfaces	Kevin (Montana)	Mill Creek	Highwood River	Sullivan Creek	Sheep River
	Clioscaphites saxitonianus	*Scaphites* (*S.*) *depressus*			
SS0					?
CS23					
CS22					
CS21					
CS20					
CS19					
CS18					
CS17					
CS16					*Sphenoceramus subcardissoides* *Volviceramus stotti,* sp. nov. *Scaphites* (*S.*) *depressus*
CS15	*Scaphites* (*S.*) *depressus*				*Scaphites* (*S.*) *depressus*
CS14					*Volviceramus cardinalensis* *Volviceramus involutus* *Volviceramus stotti,* sp. nov.
CS13					
CS12				*Volviceramus exogyroides*	
CS11					
CS10	*Volviceramus involutus* *Volviceramus koeneni*	*Scaphites* (*S.*) *ventricosus*			
CS9				*Volviceramus koeneni*	
CS8					*Volviceramus exogyroides*
CS7					*Volviceramus* sp. A
CS6					
CS5					*Volviceramus undabundus* *Scaphites* (*S.*) *ventricosus*
CS4	*Cremnoceramus crassus*		*Cremnoceramus* sp.	*Cremnoceramus* sp.	*Inoceramus gibbosus*
CS3	*Cremnoceramus crassus*				
CS2		*Scaphites* (*S.*) *preventricosus*			
CS1		*C. crassus-inconstans* lineage *Tethyoceramus ernsti* *Tethyoceramus* sp. *S.* (*S.*) *preventricosus*	*Cremnoceramus crassus crassus*		*Cremnoceramus deformis deformis*
E7		*S.* (*S.*) *preventricosus*			

Shaded area represents section not deposited, or removed below various erosion surfaces, particularly surface CS23 (maximum regressive surface).

Oldfort Creek	Burnt Timber Creek	James River	Ram River	Lynx Creek
		Clioscaphites saxitonianus		
?		*Sphenoceramus* sp. *Scaphites* (*S.*) *depressus*	*S. subcardissoides* *Sphenoceramus* sp. *Scaphites* (*S.*) *depressus*	*Sphenoceramus* sp.
			Scaphites (*S.*) *depressus*	
			Inoceramus stantoni *Volviceramus involutus*	
			S. subcardissoides *Volviceramus involutus* *Scaphites* (*S.*) *depressus* *Scaphites* (*S.*) *ventricosus*	
?		*Volviceramus* sp.		Not exposed
	Inoceramus undabundus	*Volviceramus* sp.		
Volviceramus koeneni				
Scaphites (*S.*) *ventricosus*		*Volviceramus exogyroides*		
Volviceramus sp.			*Volviceramus involutus*	
	Volviceramus tenuirostratus	*Scaphites* (*S.*) *ventricosus*	*Volviceramus involutus*	
Volviceramus involutus				
	Scaphites (*S.*) *ventricosus*			
Scaphites (*S.*) *preventricosus*				
			Cremnoceramus crassus	

Cripple Creek	Bighorn Dam	Bighorn River	Blackstone River
Sphenoceramus ex. gr. *pachti* *Clioscaphites saxitonianus*	*Sphenoceramus* ex. gr. *pachti*		
Scaphites (*S.*) *depressus*	*Volviceramus stotti,* sp. nov.	*Scaphites* (*S.*) *depressus* *Baculites* sp.	
	Scaphites (*S.*) *depressus*	*Scaphites* (*S.*) *depressus*	
	Volviceramus sp. *Scaphites* (*S.*) *depressus*	*Volviceramus* sp.	
	Volviceramus stotti, sp. nov. *Scaphites* (*S.*) *depressus* *Sphenoceramus subcardissoides* *S* (*S.*) *ventricosus* *Volviceramus cardinalensis,* sp. nov. *Inoceramus undabundus* *Volviceramus* sp.	*Baculites* sp. *Scaphites* (*S.*) *depressus* *Scaphites* (*S.*) *ventricosus*	
	Scaphites (*S.*) *ventricosus*	*Volviceramus exogyroides* *Volviceramus* sp.	
	Volviceramus exogyroides *Scaphites* (*S.*) *ventricosus*		
	Volviceramus cardinalensis, sp. nov. *Volviceramus exogyroides*		
	Volviceramus exogyroides *Inoceramus undabundus*		
	Volviceramus exogyroides		
	Volviceramus exogyroides *Inoceramus undabundus* *Volviceramus involutus* *Volviceramus tenuirostratus* *Scaphites* (*S.*) *ventricosus*		
	Volviceramus cardinalensis, sp. nov. *S.* (*S.*) *ventricosus* *Volviceramus exogyroides* *Volviceramus involutus*		
	Volviceramus cardinalensis sp. nov. *Volviceramus exogyroides* *Inoceramus undabundus* *Volviceramus involutus* *Scaphites* (*S.*) *ventricosus*	*Volviceramus exogyroides* *Volviceramus involutus*	
	Volviceramus exogyroides		
	Volviceramus cardinalensis, sp. nov. *Volviceramus exogyroides* *Inoceramus kleini*		
	Volviceramus cardinalensis, sp. nov. *Inoceramus undabundus* *Scaphites* (*S.*) *ventricosus* *Volviceramus* sp.		
	Inoceramus wandereri *Cremnoceramus* sp.		*Inoceramus gibbosus*
			Cremnoceramus deformis/ crassus *Cremnoceramus c. inconstans* *Inoceramus gibbosus*
Tethyoceramus sp. *Cremnoceramus crassus*	*Cremnoceramus crassus* *Tethyoceramus* sp. *Cremnoceramus deformis deformis* *Scaphites* (*S.*) *preventricosus*		*Cremnoceramus deformis/ crassus* *Cremnoceramus crassus inconstans*

Not exposed

Not exposed

Chungo Creek	"Brown Creek" (no identifiable fossils)	Wapiabi Creek	Cardinal River	Thistle Creek East
	Not exposed		*Sphenoceramus pachti* *Sphenoceramus* sp. *Clioscaphites saxitonianus* *Scaphites* (*S.*) *depressus*	
			Sphenoceramus subcardissoides	
				Volviceramus sp. *Scaphites* (*S.*) *depressus*
			Volviceramus involutus *Scaphites* (*S.*) *depressus*	*Volviceramus* sp.
Sphenoceramus subcardissoides				
		Volviceramus sp.		
Volviceramus involutus				
				Volviceramus sp.
Volviceramus exogyroides *Volviceramus* sp.				
Volviceramus exogyroides			*Volviceramus* sp.	
Volviceramus sp. A				
Volviceramus koeneni *Volviceramus* sp. *Scaphites* (*S.*) *ventricosus*				
Volviceramus koeneni *Scaphites* (*S.*) *ventricosus*		*Volviceramus* sp.		*Scaphites* (*S.*) *ventricosus*
Baculites sp. *Inoceramus gibbosus*		*Inoceramus gibbosus* *Inoceramus* ex. gr. *lamarcki*		
Cremnoceramus sp. *Inoceramus gibbosus*		*Inoceramus gibbosus*		
Cremnoceramus sp. *Inoceramus gibbosus*		*Cremnoceramus crassus inconstans* *Cremnoceramus* sp. *Scaphites* (*S.*) *preventricosus*		Not exposed
		Cremnoceramus crassus inconstans *Scaphites* (*S.*) *preventricosus*		

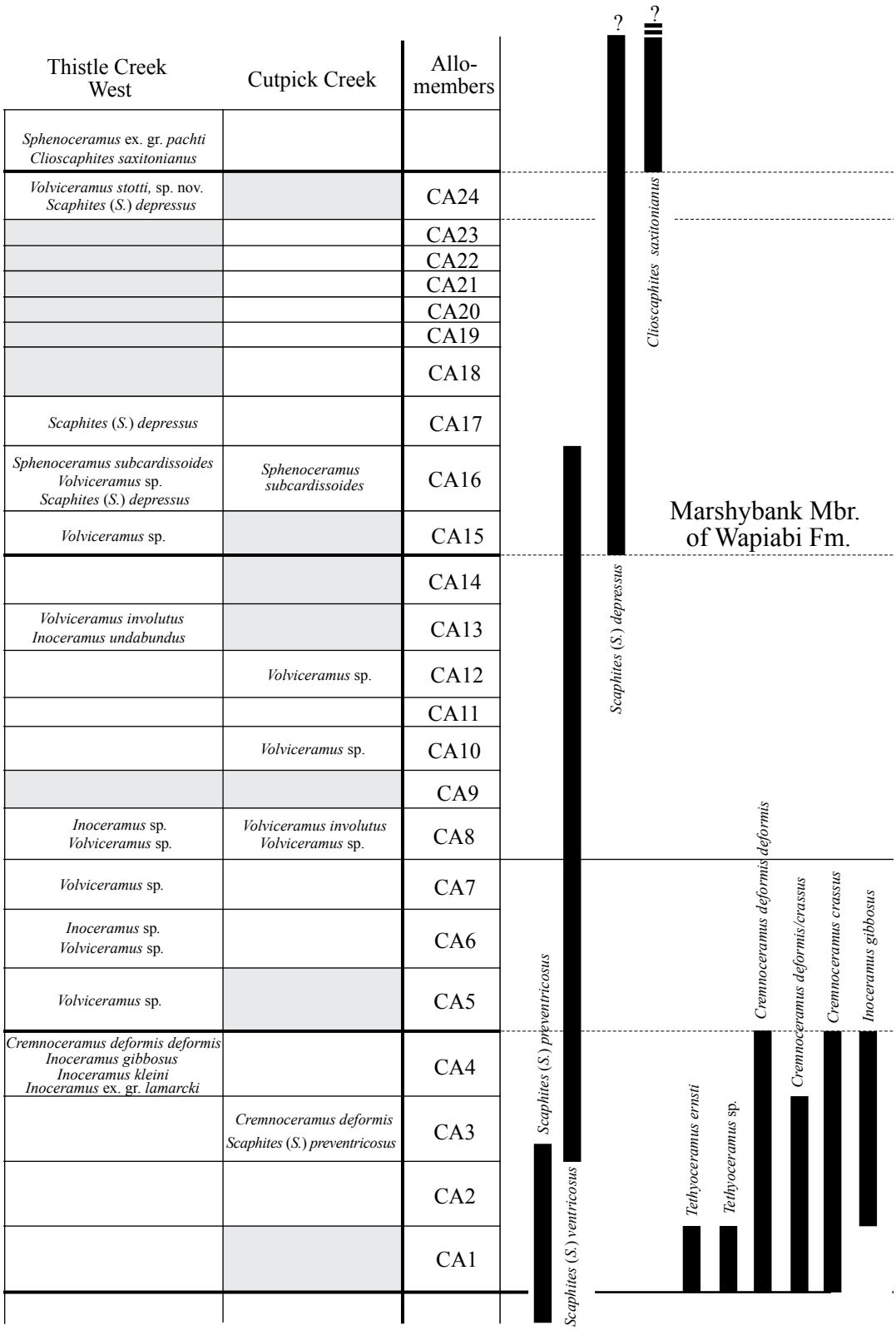
Thistle Creek West
Cutpick Creek
Allo-members
Sphenoceramus ex. gr. pachti
Clioscaphites saxitonianus
Volviceramus stotti, sp. nov.
Scaphites (S.) depressus
Scaphites (S.) depressus
Sphenoceramus subcardissoides
Volviceramus sp.
Scaphites (S.) depressus
Sphenoceramus subcardissoides
Volviceramus sp.
Volviceramus involutus
Inoceramus undabundus
Volviceramus sp.
Volviceramus sp.
Inoceramus sp.
Volviceramus sp.
Volviceramus involutus
Volviceramus sp.
Volviceramus sp.
Inoceramus sp.
Volviceramus sp.
Volviceramus sp.
Cremnoceramus deformis deformis
Inoceramus gibbosus
Inoceramus kleini
Inoceramus ex. gr. lamarcki
Cremnoceramus deformis
Scaphites (S.) preventricosus
CA24
CA23
CA22
CA21
CA20
CA19
CA18
CA17
CA16
CA15
CA14
CA13
CA12
CA11
CA10
CA9
CA8
CA7
CA6
CA5
CA4
CA3
CA2
CA1
?
?
Clioscaphites saxitonianus
Scaphites (S.) depressus
Marshybank Mbr. of Wapiabi Fm.
Scaphites (S.) preventricostus
Scaphites (S.) ventricostus
Tethyoceramus ernsti
Tethyoceramus sp.
Cremnoceramus deformis deformis
Cremnoceramus deformis/crassus
Cremnoceramus crassus
Inoceramus gibbosus

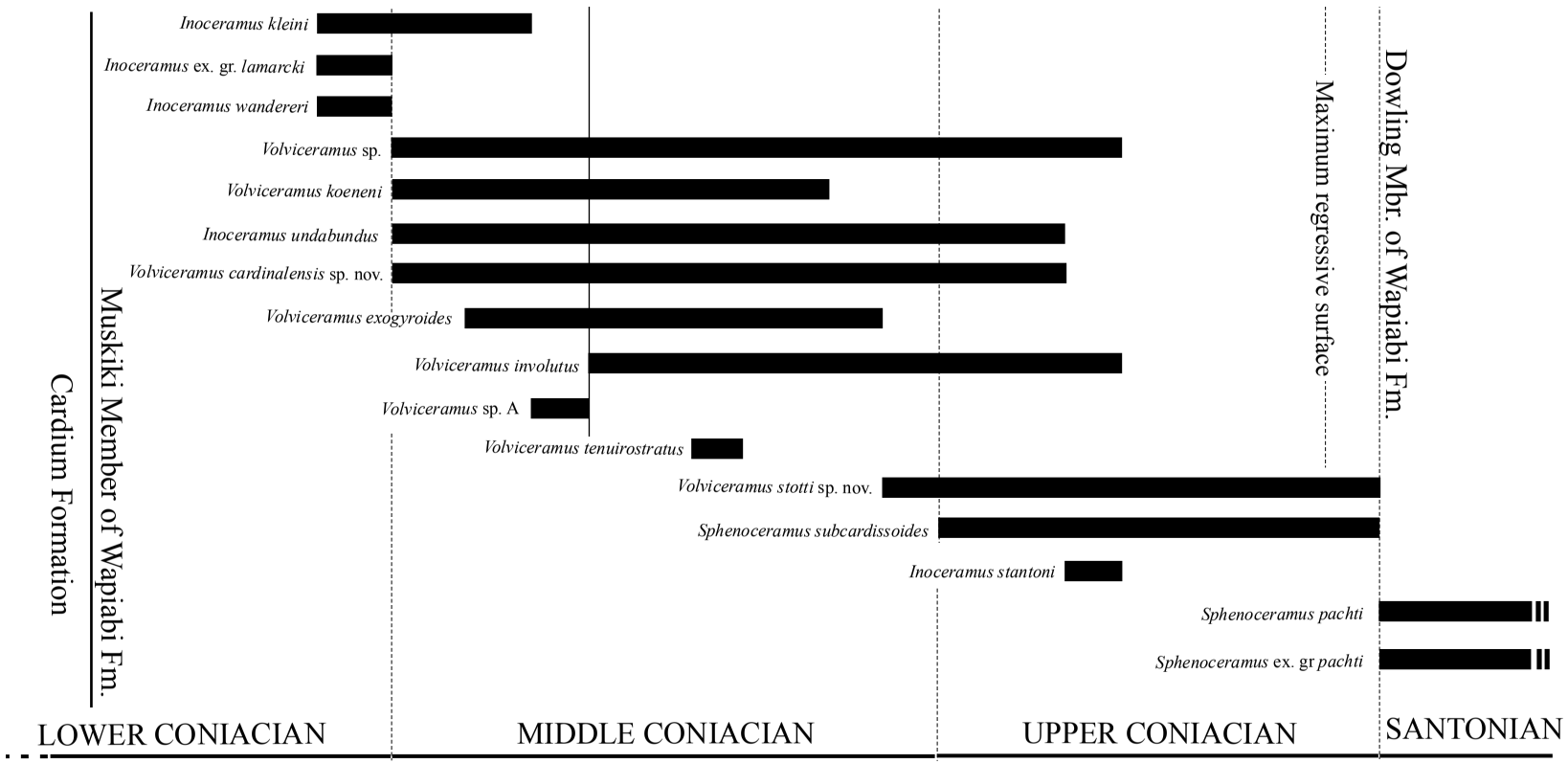
Inoceramus kleini
Inoceramus ex. gr. lamarcki
Inoceramus wandereri
Volviceramus sp.
Volviceramus koeneni
Inoceramus undabundus
Volviceramus cardinalensis sp. nov.
Volviceramus exogyroides
Volviceramus involutus
Volviceramus sp. A
Volviceramus tenuirostratus
Volviceramus stotti sp. nov.
Sphenoceramus subcardissoides
Inoceramus stantoni
Sphenoceramus pachti
Sphenoceramus ex. gr pachti
Maximum regressive surface
Dowling Mbr. of Wapiabi Fm.
Muskiki Member of Wapiabi Fm.
Cardium Formation
LOWER CONIACIAN
MIDDLE CONIACIAN
UPPER CONIACIAN
SANTONIAN

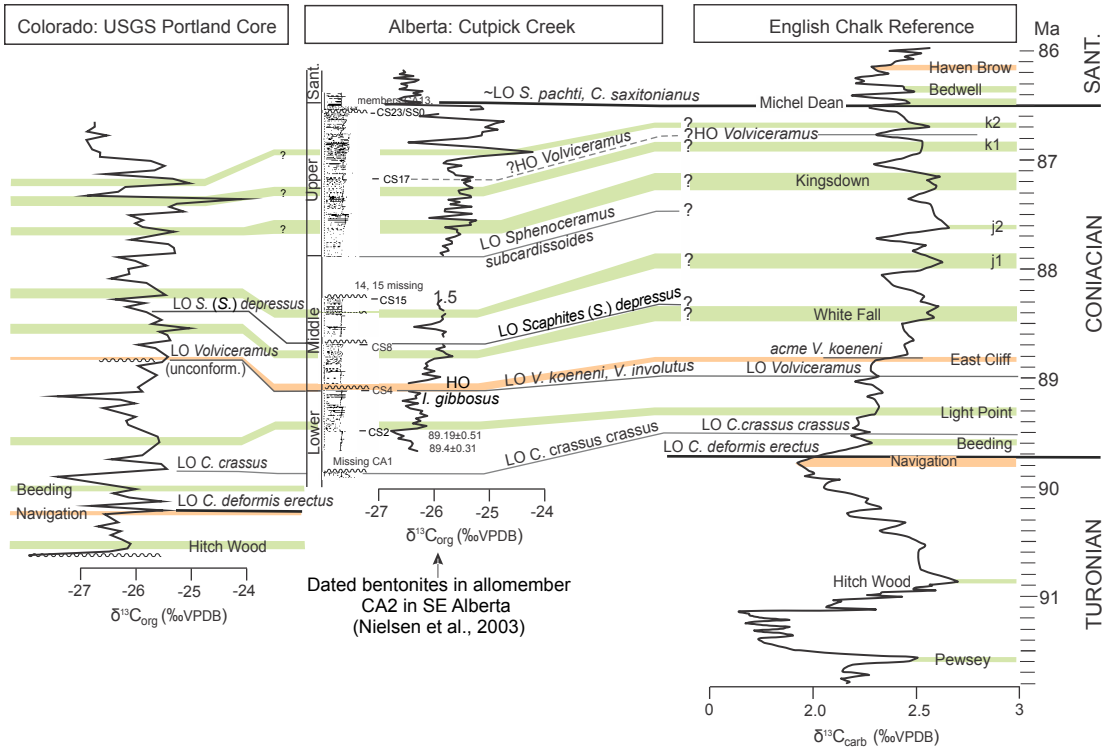

FIG. 25. Comparison of the organic carbon isotope stratigraphy at Cutpick Creek with the carbonate carbon isotope reference curve for the English Chalk succession (after Jarvis et al., 2006, recalibrated to GTS2012 after Laurin et al., 2015). The Cutpick section, and corresponding carbon-isotope curve, has been "expanded" to show the location of hiatuses determined on the basis of regional subsurface correlation (i.e., fig. 4). Biostratigraphic collections made in all the Coniacian sections included in this study (fig. 24), allow three tiepoints to the UK Chalk to be established at the lowest occurrence (LO) of *Cremnoceramus crassus crassus,* and the lowest occurrence of *Volviceramus*. The base of the Santonian is defined at the co-appearance level of *Clioscaphites saxitonianus* and *Sphenoceramus* ex gr. *pachti*, which corresponds to surface SS0 of this study. The lowest occurrence of *C. crassus*, *Volviceramus* and *Scaphites* (*S.*) *depressus* allows tentative correlation to the Portland core, which does not extend as high as the Coniacian–Santonian boundary (Joo and Sageman, 2014). The highest local occurrence of *Inoceramus gibbosus*, which is widely distributed in allomembers CA3 and CA4 in the western Alberta foredeep, is marked by the lag-strewn erosion surface CS4, suggestive of significant sea-level fall and subsequent transgression. The absence of the *I.* ex gr. *gibbosus* interval in most sections of topmost lower Coniacian strata in other parts of the world suggests that a significant hiatus exists at the base of the overlying *Volviceramus* Zone.

a broadly saucer-shaped, SW-thickening basin that thins toward both the NW and SE; this depocenter appears to have been active for about 500,000 yr. Middle Coniacian rocks (allomembers CA5–CA14) occupy a SW-thickening basin that underwent active subsidence for about 1.5 m.y. Toward the NW part of that basin, allomembers CA11–CA14 are progressively truncated by surface CS15 (fig. 4). Upper Coniacian rocks, constituting allomembers CA15–CA23, occupy a distinct northern basin that subsided for about 1 m.y; Upper Coniacian strata are truncated toward the SE by surface CS23. It is clear, therefore, that during the Coniacian the location of the active flexural depocenter shifted episodically along strike by several hundred km. Each actively subsiding basin was rimmed by a corresponding peripheral region of subtle upwarp and stratal truncation. This pattern of shifting depocenters is directly analogous to that mapped in overlying Santonian–Campanian strata (Hu and Plint, 2009; Plint et al., 2012a). The episodic subsidence of discrete, arcuate depocenters may have been a response to the development of localized salients in the adjacent deformed belt. Such salients may have developed in response to a locally thicker sedimentary cover succession, a locally weaker detachment, or a localized indentor, amongst other reasons (cf. Macedo and Marshak, 1999).

Origin of Allomembers

The excellent subsurface control available in the study area has allowed 24 Coniacian allomembers to be mapped with confidence. Allomembers are typically <10 m thick, and rarely exceed 20 m (figs. 4–13), yet can be traced along and across strike for hundreds of km. Given the ~3.0 m.y. represented by the studied interval of strata, each of the 24 allomembers can be inferred to have had an average duration of ~125,000 yr. The ubiquitous upward-coarsening signature of allomembers, coupled with the widespread presence of intra- or extrabasinal pebble lags on flooding surfaces, indicates that many allomembers can be interpreted as depositional sequences, each of which embodies evidence for initial relative sea-level rise, followed by shoaling, and terminated by relative sea-level fall that led to erosion of the sea floor, and in some cases, to subaerial emergence. The lateral continuity, over hundreds of km, coupled with the extremely high aspect-ratio of each allomember suggests that depositional cyclicity was a response to allogenic forcing, rather than to localized autogenic effects such as delta lobe switching. It is possible that depositional cyclicity was the result of changes in the rate of clastic sediment supply that resulted in alternating coastal progradation and transgression, manifest as upward-shoaling successions bounded by flooding surfaces. However, extrabasinal pebble lags imply episodes of relative sea-level fall and subaerial exposure that can not be explained solely in terms of a changing rate of sediment supply.

Relative sea-level rise and fall can be effected by both tectonic and eustatic mechanisms. The stratigraphic data presented herein (figs. 4–13, 26), provide evidence that stratal packages composed of several allomembers form large-scale arcuate wedges that are most reasonably explained in terms of differential flexural subsidence and uplift on length scales of hundreds of kilometers. This pattern contrasts sharply with the relatively tabular geometry of individual allomembers. Given the evidence that tectonic subsidence due to static loading resulted in broad, saucer-shaped depocenters, it seems difficult to also attribute the tabular geometry of allomembers to the same mechanism. Allomembers are therefore most simply explained as a consequence of relatively high-frequency (order of 100,000 yr) eustatic sea-level cycles superimposed on relatively low-frequency (order of 0.5 to 1.5 m.y.), and spatially non-uniform pulses of tectonically driven subsidence.

Nature of Biozonal Boundaries

Important biotic colonization events that mark the lowest occurrences of *Cremnoceramus crassus crassus*, *Volviceramus*, *Sphenoceramus subcardissoides,* and *S. pachti*, all correspond to widely mappable erosion surfaces that indicate relative sea-level fall followed by transgression. Sea-level changes therefore appear to have played

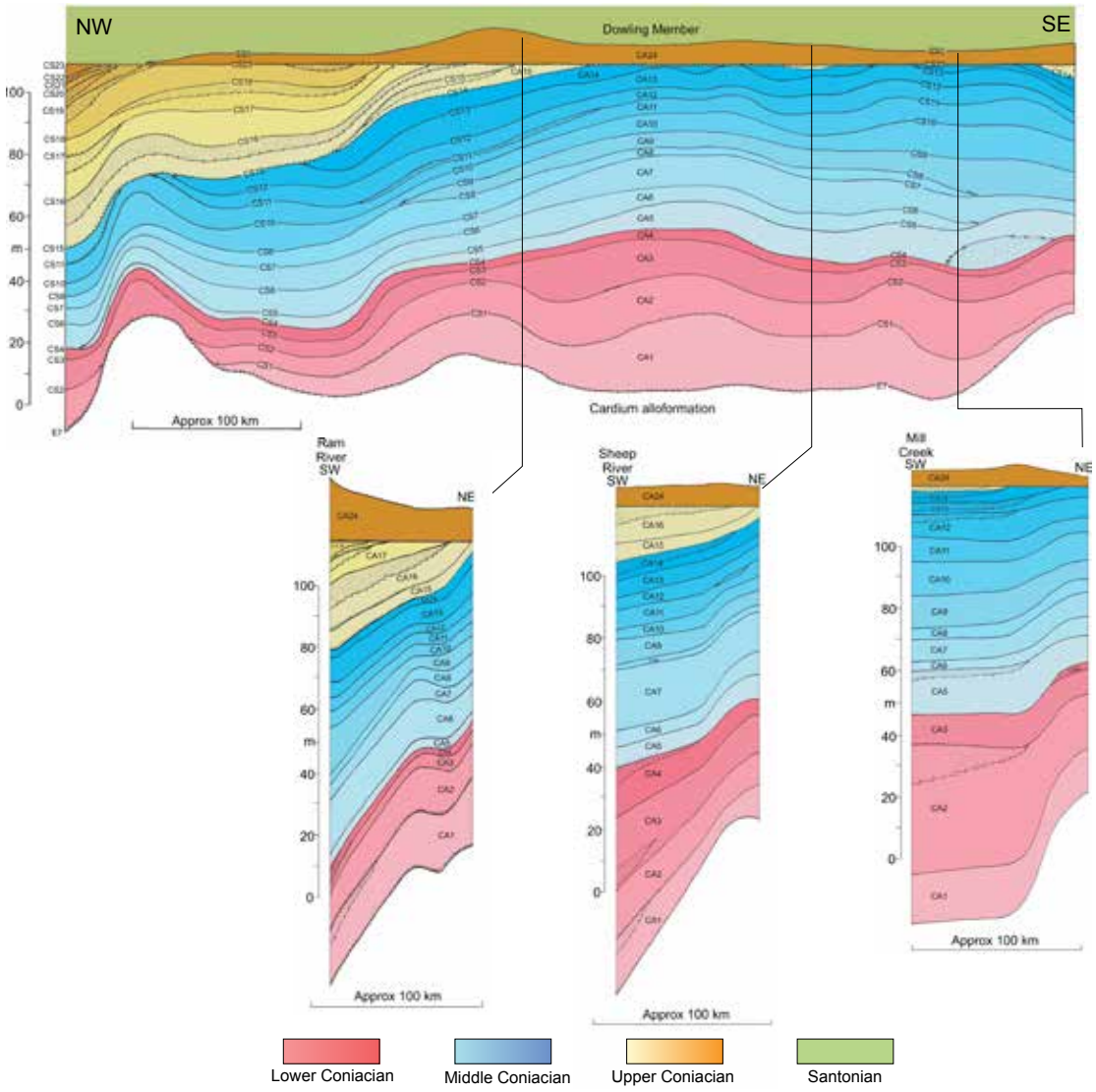

FIG. 26. Summary representation, to scale, of stratal geometry viewed in strike (NW-SE) and three dip (NE-SW) sections spanning the study area. Lower Coniacian strata fill a saucer-shaped depocenter that thins to both NW and SE, whereas Middle Coniacian strata are thickest in the south but are erosionally truncated toward the NW. Upper Coniacian strata fill a depocenter in the NW but are truncated toward the SE, and are largely absent over most of southern Alberta and northern Montana. Sections summarized from figures 4, 8, 11, and 13.

an important role in speciation and extinction events. Because marine flooding surfaces can be considered to have formed geologically instantaneously, it is also reasonable to interpret the boundaries of the inoceramid biozones to closely approximate time planes.

The coincidence between the lowest and highest occurrences of scaphitid ammonite species and erosional surfaces subsequently modified by transgression is less clear. The lowest occurrence of *Scaphites* (*S.*) *preventricosus* is just above erosional surface E5.5, which marks the beginning of a major transgression (Walaszczyk et al., 2014). However, the lowest occurrence of *S.* (*S.*) *ventricosus* is immediately above surface CS2, in allomember CA3, close to an interpreted highstand. The lowest occurrence of *S.* (*S.*) *depressus* is just above surface CS14, which marks a high-frequency flooding surface during a long-term shallowing trend that continued, punctuated by minor transgressions, through much of the late Coniacian. In contrast, the lowest occurrence of *Clioscaphites saxitonianus* is at the base of the Santonian (surface SS0), coinciding with a major transgression and a marked change in facies to deeper-water, more offshore mudstones.

CONCLUSIONS

1. Coniacian marine rocks within a >750 km transect along the foredeep of the Western Canada Foreland Basin have been divided into a succession of 24 allomembers, bounded by marine flooding surfaces. Flooding surfaces have been correlated through a grid of ~4,800 wireline well logs, embracing an area of about 200,000 km^2, and have also been traced into equivalent strata exposed in the fold-and-thrust belt on the western margin of the basin.
2. Flooding surfaces probably formed on a time scale of only a few thousand years, and hence can be treated as proxy time lines. The allostratigraphic framework therefore provides a near-chronostratigraphic framework within which to analyze spatial and temporal patterns of molluscan evolution.
3. In the study area, Coniacian rocks are divided into five broad facies that represent a spectrum of offshore to shoreface environments. Offshore sediments are mudstones and siltstones with abundant wave ripples that indicate deposition above storm-wave base (probably only a few tens of m deep). Bioturbation intensity varies from 0 to 6. Low bioturbation index is attributed primarily to a low (2–5 mg/L^{-1}) dissolved oxygen content in bottom water, insufficient to support a benthic macrofauna; intensely bioturbated sediments indicate better oxygenated conditions. Sediments deposited closer to shore include variably bioturbated siltstones and sandstones with wave ripples and HCS, whereas mud-free sandstone with SCS represents a storm-influenced shoreface.
4. Flooding surfaces may lack a coarse-grained lag, or may bear anomalously coarse sand or pebbles. Pebbles may be intraformational clasts of siderite or phosphate or extrabasinal chert. Siderite and phosphate pebbles indicate erosion of the sea floor sufficient to exhume early diagenetic nodules, but do not prove subaerial emergence. Chert pebbles must have been supplied by rivers and imply a period of subaerial emergence of the shelf prior to transgressive reworking.
5. The more mudstone-rich facies contain abundant inoceramid bivalve and scaphitid ammonite fossils, preserved mainly as uncompressed siderite infills of the shell. Fossils were located precisely in measured outcrop sections, and subsequently were correlated into the regional subsurface allostratigraphic framework.
6. Several major speciation events among inoceramids are recognized. The lowest occurrence of *Cremnoceramus crassus crassus* coincides with the E7 surface at the base of the Muskiki Member; the fauna persists up to surface CS4. The *Inoceramus gibbosus* group is present only in allomembers CA2–

CA4 but is not found above surface CS4, which marks the Lower to Middle Coniacian boundary. Immediately above surface CS4 appear various species of *Volviceramus,* which rapidly become abundant. *Sphenoceramus subcardissoides* appears in allomember CA15 together with *Scaphites* (*S.*) *depressus* and hence marks the base of the upper Coniacian. *Sphenoceramus pachti,* together with *Clioscaphites saxitonianus* appear immediately above surface SS0 and mark the base of the Santonian.

7. The lowest occurrence of *Scaphites* (*S.*) *preventricosus* is just above Cardium Formation erosion surface E5.5, which lies just below the base of the Coniacian. The lowest occurrence of *S.* (*S.*) *ventricosus* is immediately above surface CS2 in allomember CA3, which is a short distance below the base of the Middle Coniacian. The lowest occurrence of *S.* (*S.*) *depressus* is in allomember CA15, immediately above surface CS 14, which marks both the onset of major regression and the base of the upper Coniacian. The lowest occurrence of *Clioscaphites saxitonianus* is at transgressive surface SS0, which marks the local base of the Santonian.
8. The close correspondence between marine transgressive events and the appearance of new inoceramid (and sometimes ammonite) species suggests that the evolution and dispersal of new inoceramid species took place during episodes of relative sea-level rise that in some cases were preceded by a distinct lowstand.
9. A preliminary carbon-isotope record was obtained for Coniacian strata at Cutpick Creek in west-central Alberta. The succession of carbon-isotope events (CIE) are tentatively correlated to the English Chalk reference curve. The Light Point, East Cliff, and White Fall CIE appear to be recognizable with some degree of confidence. The carbon-isotope record at Cutpick Creek is also tentatively correlated with the Coniacian isotope record from hemipelagic sediments in Colorado, where biostratigraphic control from the lowest occurrences of *Volviceramus* and *Scaphites* (*S.*) *depressus* allows tentative correlation of the Light Point, East Cliff, and White Fall CIE.
10. Mapping of allomembers along the strike of the foredeep shows that allomembers can be grouped into natural "tectono-stratigraphic" units that span ca. 0.5 to 1.5 m.y., and are bounded by low-angle bevelling unconformities that truncate packages of nearly tabular allomembers. Each tectono-stratigraphic unit fills a broadly saucer-shaped depocenter, interpreted to have subsided in response to active tectonic loading in the adjacent sector of the fold-and-thrust belt.
11. The astronomically calibrated succession of CIE in the English Chalk provides an absolute time scale against which to interpret transgressive-regressive events in Alberta. The 24 mapped allomembers appear to span close to 3.0 m.y., suggesting that on average, each allomember represents about 125,000 yr. Because the flooding surfaces that bound allomembers can be mapped for hundreds of km (and in cases >1000 km), an at least regional-scale allogenic control is indicated: high-frequency eustatic change appears to provide the most likely driving mechanism.
12. Toward the south, upper Coniacian strata are progressively bevelled off such that south of about latitude 51° N, the succession comprises primarily lower and middle Coniacian strata, and most late Coniacian time is represented by an erosion surface, mantled by 0.1 to 1.2 m of chert-pebble bearing ooidal ironstone. This ironstone is correlative with the MacGowan Concretionary Bed mapped over much of western Montana. The region of late Coniacian uplift in southern Alberta probably constitutes a peripheral bulge related to a late Coniacian flexural depocenter located in NE British Columbia.

ACKNOWLEDGMENTS

The results reported here are based on 16 summers of fieldwork by the senior author and graduate students B. Norris, J. McKay, S. Donaldson, M. Grifi and E. Hooper, in collaboration with Dr. I. Walaszczyk. We were ably assisted in the field by O. Al-Mufti, P. Angiel, R. Buckley, S. CoDyer, R. Cotton-Barratt, P. Elliott, B. Hart, Y. Hu, S. Morrow, M. O'Driscoll, K. Pavan, T. Plint, J. Shank, K. Vannelli, and R. Vesely. Funding for A.G.P.'s regional stratigraphic studies was provided by the Natural Sciences and Engineering Research Council of Canada, over numerous grant cycles. Supplementary funding was provided by Canadian Hunter Ltd, Home Oil Ltd., Imperial Oil Ltd., Texaco Ltd., and Unocal Canada, Ltd. Well-log data were donated by Imperial Oil Ltd and Divestco Ltd. A gamma-ray spectrometer was donated by the former PanCanadian Petroleum Ltd. I.W. acknowledges the financial support of the Faculty of Geology of the University of Warsaw (BST grant No. 173502). D.R.G. and I.J. acknowledge funding by UK Natural Environment Research Council (NERC) grants NE/H021868/1 and NE/H020756/1, respectively.

N.H.L. thanks Mary Conway (AMNH) for curation of the specimens, Stephen Thurston (AMNH) for photographing the specimens and preparing the figures, Mariah Slovacek (AMNH), and Neal Larson (Larson Paleontology Unlimited, Keystone, SD) for preparation of the specimens, and Brandon Strilisky (TMP) for facilitating the accession of the specimens into the Tyrell Museum of Paleontology. We express our thanks to Ben Hathway and Matthew P. Garb for their detailed and perceptive comments that significantly improved the final text.

REFERENCES

Benyon, C., et al. 2014. Provenance of the Cretaceous Athabasca Oil Sands, Canada: implications for continent-scale sediment transport. Journal of Sedimentary Research 84: 136–143.

Bhattacharya, J.P., and R.G. Walker. 1991a. Allostratigraphic subdivision of the Upper Cretaceous Dunvegan, Shaftesbury and Kaskapau formations in the northwestern Alberta subsurface. Bulletin of Canadian Petroleum Geology 39: 145–164.

Bhattacharya, J.P., and R.G. Walker. 1991b. River- and wave-dominated depositional systems of the Upper Cretaceous Dunvegan Formation, northwestern Alberta. Bulletin of Canadian Petroleum Geology 39: 165–191.

Blum, M., and M. Pecha. 2014. Mid-Cretaceous to Paleocene North American drainage reorganization from detrital zircons. Geology 42: 607–610.

Buckley, R.A., A.G. Plint, O.A. Henderson, J.R. Krawetz, and K.M. Vannelli. 2016. Ramp sedimentation across a middle Albian, Arctic embayment: influence of subsidence, eustasy and sediment supply on stratal architecture and facies distribution, Lower Cretaceous, Western Canada Foreland Basin. Sedimentology 63: 699–742.

Catuneanu, O. 2006. Principles of sequence stratigraphy. Amsterdam: Elsevier, 375 p.

Cheel, R.J., and D.A. Leckie. 1993. Hummocky cross-stratification. Sedimentology Review 1: 103–122. Oxford: Blackwell Scientific.

Clifton, H.E. 2006. A reexamination of facies models for clastic shorelines. *In* H.W. Posamentier and R.G. Walker (editors), Facies models revisited. SEPM (Society for Sedimentary Geology) Special Publication 84: 293–337.

Cobban, W.A., C.E. Erdmann, R.W. Lemke, and F.K. Maughan. 1959. Revision of Colorado Group on Sweetgrass Arch, Montana. American Association of Petroleum Geologists, Bulletin 43: 2786–2796.

Cobban, W.A., C.E. Erdmann, R.W. Lemke, and E.K. Maughan, E.K. 1976. Type sections and stratigraphy of the Blackleaf and Marias River formations (Cretaceous) of the Sweetgrass Arch, Montana. United States Geological Survey, Professional Paper 974: 1–66.

Cobban, W.A., T.S. Dyman, and K.W. Porter. 2005. Paleontology and stratigraphy of upper Coniacian–middle Santonian ammonite zones and application to erosion surfaces and marine transgressive strata in Montana and Alberta. Cretaceous Research 26: 429–449.

Collom, C.J. 2001. Systematic paleontology, biostratigraphy, and paleoenvironmental analysis of the Wapiabi Formation (Upper Cretaceous), Alberta and British Columbia, Western Canada. Ph.D. dissertation, University of Calgary, Alberta, 834 pp.

Cross, T.A., and M.A. Lessenger. 1988. Seismic stratigraphy. Annual Review of Earth and Planetary Sciences 16: 319–354.

Dashtgard, S.E., and J.A. MacEachern. 2016. Unburrowed mudstones may record only slightly lowered oxygen conditions in warm, shallow basins. Geology 44: 371–374.

Dashtgard, S.E., J.W. Snedden, and J.A. MacEachern. 2015. Unbioturbated sediments on a muddy shelf: hypoxia or simply reduced oxygen saturation? Palaeogeography, Palaeoclimatology, Palaeoecology 425: 128–138.

Donaldson, W.S. 1997. The sedimentology, stratigraphy and diagenesis of the Upper Cretaceous Bad Heart Formation, NW Alberta. Ph.D. dissertation, University of Western Ontario, London, 492 pp.

Donaldson, W.S., A.G. Plint, and F.J. Longstaffe. 1998. Basement tectonic control on the distribution of the shallow marine Bad Heart Formation: Peace River Arch area, NW Alberta. Bulletin of Canadian Petroleum Geology 46: 576–598.

Donaldson, W.S., A.G. Plint, and F.J. Longstaffe. 1999. Tectonic and eustatic control on deposition and preservation of Upper Cretaceous ooidal ironstone and associated facies: Peace River Arch area, NW Alberta, Canada. Sedimentology 46: 576–598.

Durbano, A. 2009. Stratigraphy of the Muskiki and Marshybank formations (Coniacian), west-central Alberta. B.Sc. thesis, University of Western Ontario, London, 48 pp.

Evenchick, C.A., M.E. McMechan, V.J. McNichol, and S.D. Carr, S.D. 2007. A synthesis of the Jurassic-Cretaceous tectonic evolution of the central and southeastern Canadian Cordillera: Exploring links across the orogen. *In* J.W. Sears, T.A. Harms and C.A. Evenchick (editors), Whence the mountains? Inquiries into the evolution of orogenic systems: a volume in honor of Raymond A. Price. Geological Society of America, Special Paper 433: 117–145.

Grifi, M.D. 2012. Stratigraphy and sedimentology of the Late Cretaceous (Coniacian) Muskiki and Marshybank members, southern Alberta and northwestern Montana. M.Sc. thesis, University of Western Ontario, London, 216 pp.

Grifi, M.D., A.G. Plint, and I. Walaszczyk. 2013. Rapidly changing styles of subsidence revealed by high-resolution mudstone allostratigraphy: Coniacian of Sweetgrass Arch area, southern Alberta and northern Montana. Canadian Journal of Earth Sciences 50: 439–461.

Hooper, E. In prep. Allostratigraphy and sedimentology of the Muskiki and Marshybank members (Late Cretaceous, Coniacian) in southwestern Alberta, Canada. Ph.D. dissertation, University of Western Ontario, London.

Hooper, E., and A.G. Plint. 2016. Cryptic migrating depocentres in a mudstone-dominated succession: Coniacian Muskiki and Marshybank members, Central Alberta Plains and Foothills, Western Canada Foreland Basin. AAPG Annual Convention, Calgary, June 19–23, 2016. Poster, abstract on line.

Hu, Y.G., and A.G. Plint, A.G. 2009. An allostratigraphic correlation of a mudstone-dominated syntectonic wedge: the Puskwaskau Formation (Santonian-Campanian) in outcrop and subsurface, Western Canada foreland basin. Bulletin of Canadian Petroleum Geology 57: 1–33.

Jarvis, I., A.S. Gale, H.C. Jenkyns, and M.A. Pearce. 2006. Secular variation in Late Cretaceous carbon isotopes: a new $\delta^{13}C$ carbonate reference curve for the Cenomanian-Campanian (99.6–70.6 Ma). Geological Magazine 143: 561–608.

Jarvis, I., J. Trabucho-Alexandre, D.R. Gröcke, D. Uličný, and J. Laurin. 2015. Intercontinental correlation of organic carbon and carbonate stable isotope records: evidence of climate and sea-level change during the Turonian (Cretaceous). Depositional Record 1: 53–90.

Joo, Y.J., and B.B. Sageman. 2014. Cenomanian to Campanian carbon isotope chemostratigraphy from the Western Interior Basin, USA. Journal of Sedimentary Research 84: 529–542.

Kafle, B., R.A. Olson, and O. Catuneanu. 2013. Stratigraphy of the Bad Heart Formation, Clear Hills and Smoky River areas, Alberta. Bulletin of Canadian Petroleum Geology 61: 253–282.

Kauffman, E.G. 1977. Geological and biological overview: Western Interior Cretaceous Basin. Mountain Geologist 14: 75–99.

Kennedy, W.J., and W.A. Cobban. 1991. Coniacian ammonite faunas from the United States Western Interior. Special Papers in Palaeontology 45: 1–96. [London]: Palaeontological Association.

Laurin, J., S.R. Meyers, D. Uličný, I. Jarvis, and B.B. Sageman. 2015. Axial obliquity control on the greenhouse carbon budget through middle- to high-latitude reservoirs. Paleoceanography 30: 133–149.

Leckie, D.A., and R.J. Cheel. 1997. Sedimentology and depositional history of Lower Cretaceous coarse-grained clastics, southwest Alberta and southeast British Columbia. Bulletin of Canadian Petroleum Geology 45: 1–24.

Leier, A.L., and G.E. Gehrels. 2011. Continent-scale detrital zircon provenance signatures in Lower Cretaceous strata, western North America. Geology 39: 399–402.

MacEachern, J.A., S.G. Pemberton, M.K. Gingras, and K.L. Bann. 2010. Ichnology and facies models. *In*

R.W. Dalrymple and N.P. James (editors), Facies models 4 (GEOtext 6): 19–58. St. John's, Newfoundland: Geological Association of Canada.

Macedo, J., and S. Marshak. 1999. Controls on the geometry of fold-thrust belt salients. Bulletin of the Geological Society of America 111: 1808–1822.

Malloch, C.S. 1911. Bighorn Coal Basin, Alberta. Geological Survey of Canada Memoir 9E: 1–66.

McKay, J.L., F.J. Longstaffe, and A.G. Plint. 1995. Early diagenesis and its relationship to depositional environment and relative sea level fluctuations (Upper Cretaceous Marshybank Formation, Alberta and British Columbia). Sedimentology 42: 161–190.

NACSN (North American Commission on Stratigraphic Nomenclature). 2005. North American Stratigraphic Code. American Association of Petroleum Geologists Bulletin 89: 1547–1591.

Nielsen, K.S., C.J. Schröder-Adams, and D.A. Leckie. 2003. A new stratigraphic framework for the Upper Colorado Group (Cretaceous) in southern Alberta and southwestern Saskatchewan, Canada. Bulletin of Canadian Petroleum Geology 51: 304–346.

Nielsen, K.S., C.J. Schröder-Adams, D.A. Leckie, J.W. Haggart, and K. Elberdak. 2008. Turonian to Santonian paleoenvironmental changes in the Cretaceous Western Interior Sea: the Carlile and Niobrara formations in southern Alberta and southwestern Saskatchewan, Canada. Palaeogeography, Palaeoclimatology, Palaeoecology 270: 64–91.

Norris, B. 1989. The Upper Cretaceous Muskiki, Marshybank and Bad Heart formations (Smoky Group), Western Interior Seaway, northwestern Alberta, Canada: relative sea level control on stratigraphy and sedimentology. M.Sc. thesis, University of Western Ontario, London, 341 pp.

Obradovich, J.D., and W.A. Cobban. 1975. A time-scale for the Late Cretaceous of the Western Interior of North America. Geological Association of Canada Special Paper 13: 31–54.

Plint, A.G. 1990. An allostratigraphic correlation of the Muskiki and Marshybank formations (Coniacian–Santonian) in the foothills and subsurface of the Alberta Basin. Bulletin of Canadian Petroleum Geology 38: 288–306.

Plint, A.G. 1991. High-frequency relative sea level oscillations in Upper Cretaceous shelf clastics of the Alberta Foreland Basin: evidence for a Milankovitch-scale glacio-eustatic control? *In* D.I.M. Macdonald (editor), Sedimentation, tectonics and eustacy. International Association of Sedimentologists Special Publication 12: 409–428. Oxford: Blackwell Science.

Plint, A.G. 2000. Sequence stratigraphy and paleogeography of a Cenomanian deltaic complex: the Dunvegan and lower Kaskapau formations in subsurface and outcrop, Alberta and British Columbia, Canada. Bulletin of Canadian Petroleum Geology 47: 43–79.

Plint, A.G. 2010. Chapter 8: Wave- and storm-dominated shoreline and shallow marine systems. *In* R.W. Dalrymple and N.P. James (editors), Facies models 4 (GEOtext 6): 167–199. St. John's, Newfoundland: Geological Association of Canada.

Plint, A.G. 2014. Mud dispersal across a Cretaceous prodelta: storm-generated, wave-enhanced sediment gravity flows inferred from mudstone microtexture and microfacies. Sedimentology 61: 609–647.

Plint, A.G., and B. Norris. 1991. Anatomy of a ramp margin sequence: facies successions, paleogeography and sediment dispersal patterns in the Muskiki and Marshybank formations, Alberta Foreland Basin. Bulletin of Canadian Petroleum Geology 39: 18–42.

Plint, A.G., and D. Nummedal. 2000. The falling stage systems tract: Recognition and importance in sequence stratigraphic analysis. *In* D. Hunt and R.L.G. Gawthorpe (editors), Sedimentary responses to forced regressions. Geological Society of London Special Publication 172: 1–17.

Plint, A.G., R.G. Walker, and K.M. Bergman. 1986. Cardium Formation 6. Stratigraphic framework of the Cardium in subsurface. Bulletin of Canadian Petroleum Geology 34: 213–225.

Plint, A.G., B. Norris, and W.S. Donaldson. 1990. Revised definitions for the Upper Cretaceous Bad Heart Formation and associated units in the foothills and plains of Alberta and British Columbia. Bulletin of Canadian Petroleum Geology 38: 78–88.

Plint, A.G., et al. 2012a. Dynamic relationship between subsidence, sedimentation, and unconformities in mid-Cretaceous, shallow-marine strata of the Western Canada Foreland Basin: links to cordilleran tectonics. *In* C. Busby and A. Azor (editors), Recent advances in the tectonics of sedimentary basins: 480–507. Oxford: Wiley-Blackwell Publishing.

Plint, A.G., J.H.S. Macquaker, and B.L.Varban. 2012b. Bedload transport of mud across a wide, storm-influenced ramp: Cenomanian-Turonian Kaskapau Formation, Western Canada Foreland Basin. Journal of Sedimentary Research 82: 801–822.

Price, R.A. 1994. Chapter 2: Cordilleran tectonics and the evolution of the Western Canada Sedimentary Basin. *In* G. Mossop and I. Shetsen (compilers), Geological atlas of the Western Canada Sedimentary Basin: 13–24. Calgary: Canadian Society of Petroleum Geologists and Alberta Research Council.

Raines, M.K., S.M. Hubbard, R.B. Kukulski, A.L. Leier, and G. Gehrels. 2013. Sediment dispersal in an evolving foreland: Detrital zircon geochronology from Upper Jurassic and lowermost Cretaceous strata, Alberta Basin, Canada. Bulletin of the Geological Society of America 125: 741–755.

Roca, X., et al. 2008. An allostratigraphic correlation of Lower Colorado Group (Albian) and equivalent strata in Alberta and British Columbia, and Cenomanian rocks of the Upper Colorado Group in southern Alberta. Bulletin of Canadian Petroleum Geology 56: 259–299.

Rottenfusser, B., et al. 2002. Regional evaluation of the coalbed methane potential in the plains and foothills of Alberta, stratigraphy and rank study (digital version). Alberta Geological Survey Special Report 7: 1–248. Calgary: Alberta Energy and Utilities Board.

Sageman, B.B., et al. 2013. Integrating $^{40}Ar/^{39}Ar$, U-Pb, and astronomical clocks in the Cretaceous Niobrara Formation, Western Interior Basin, USA. Bulletin of the Geological Society of America 126: 956–973.

Schröder-Adams, C.J., J.O. Herrle, and Q. Tu. 2012. Albian to Santonian carbon isotope excursions and faunal extinctions in the Canadian Western Interior Sea: Recognition of eustatic sea-level controls on a forebulge setting. Sedimentary Geology 281: 50–58.

Seitz, O. 1959. Vergleichende Stratigraphie der Oberkreide in Deutschland und in Nordamerika mit Hilfe der Inoceramen. *In* L.B. Kellum (chairman), El Sistema Cretacico. Un symposium sobre el Cretacico en el hemisferio occidental y su correlacion mundial: vol. 1: 113–130. 20th International Geological Conference, Mexico City, Mexico,

Shank, J.A. 2012. Sedimentology and allostratigraphy of the Cardium Formation (Turonian-Coniacian) in southern Alberta and equivalent strata in northern Montana. Ph.D. dissertation, University of Western Ontario, London, 374 pp.

Shank, J.A., and A.G. Plint. 2013. Allostratigraphy of the Upper Cretaceous Cardium Formation in subsurface and outcrop in southern Alberta, and correlation to equivalent strata in northwestern Montana. Bulletin of Canadian Petroleum Geology 61: 1–40.

Stott, D.F. 1956. The Alberta Group, Rocky Mountain Foothills, Alberta. Geological Survey of Canada Paper 56-1: 1–71.

Stott, D.F. 1963. The Cretaceous Alberta Group and equivalent rocks, Rocky Mountain Foothills, Alberta. Geological Survey of Canada Memoir 317: 1–297 p.

Stott, D.F. 1967. The Cretaceous Smoky Group, Rocky Mountain Foothills, Alberta and British Columbia. Geological Survey of Canada Bulletin 132: 1–133.

Varban, B.L., and A.G. Plint. 2008a. Palaeoenvironments, palaeogeography, and physiography of a large, shallow, muddy ramp: Late Cenomanian-Turonian Kaskapau Formation, Western Canada foreland basin. Sedimentology 55: 201–233.

Varban, B.L., and A.G. Plint. 2008b. Sequence stacking patterns in the Western Canada foredeep: Influence of tectonics, sediment loading and eustasy on deposition of the Upper Cretaceous Kaskapau and Cardium formations. Sedimentology 55: 395–421.

Wadsworth, J.A., and R.G. Walker. 1991. Morphology and origin of erosion surfaces in the Cardium Formation (Upper Cretaceous, Western Interior Seaway, Alberta) and their implications for rapid sea-level fluctuations. Canadian Journal of Earth Sciences 28: 1507–1520.

Walaszczyk, I., and W.A. Cobban. 2006. Palaeontology and biostratigraphy of the Middle-Upper Coniacian and Santonian inoceramids if the US Western Interior. Acta Geologica Polonica 56: 241–348.

Walaszczyk, I., J.A. Shank, A.G. Plint, and W.A. Cobban. 2014. Inter-regional correlation of disconformities in Upper Cretaceous strata, Western Interior Seaway: biostratigraphic and sequence-stratigraphic evidence for eustatic change. Bulletin of the Geological Society of America 126: 307–316.

Wall, J.H., and R.K. Rosene. 1977. Cretaceous stratigraphy and micropaleontology of the Crowsnest Pass–Waterton area, southern Alberta Foothills. Bulletin of Canadian Petroleum Geology 25: 842–867.

Williams, G.D., and C.R. Stelck. 1975. Speculations on the Cretaceous palaeogeography of North America. *In* W.G.E. Caldwell (editor), The Cretaceous System in the Western Interior of North America. Geological Association of Canada Special Paper 13: 1–20.

Wright, G.N., M.E. McMechan, and D.E.G. Potter. 1994. Chapter 3: Structure and architecture of the Western Canada Sedimentary Basin. *In* G. Mossop and I. Shetsen (compilers), Geological Atlas of the Western Canada Sedimentary Basin: 25–40. Calgary: Canadian Society of Petroleum Geologists and Alberta Research Council.

APPENDIX 1

Location of Measured Sections in this Study, Including Reference to Available Published Accounts

Locality Name	Published Description	Canadian NTS Grid Reference Latitude, Longitude	Access
Bighorn Dam	N/A	83C/8 462953 52°18′26.30″N, 116°19′06.49″W	Walk
Bighorn River	Stott, 1963, cross section 5-38	83C/8 366038 52°23′07.0″N 116°27′46.79″W	Helicopter
Blackstone River east	N/A	83C/9 472298 52°38′20.37″N, 116°18′17.76″W	Walk
"Brown Creek" (actually an un-named tributary of Brown Creek)	Stott, 1963, pl. 27, no description.	83C/10 214416 52°43′15.13″N 116°41′08.63″W	Helicopter
Burnt Timber Creek	Stott, 1963, cross section 6-9	82O/11 257108 51°32′06.01″N 115°11′12.22″W	Walk
Cardinal River	Stott, 1963, cross section 4-31	83C/15 221578 52°52′15.73″N 116°40′30.85″W	Walk
Chungo Creek	Stott, 1963, cross section 4-8	83C/9 375383 52°41′42.68″N 116°26′51.03″W	Walk
Cripple Creek	Stott, 1963, cross section 5-42	83B/4 705844 52°12′27.35″N 115°58′02.85″W	Walk
Cutpick Creek	Close to Stott, 1967, cross section 58-2	83L/3 605924 54°03′42.56″N 119°07′58.98″W	Helicopter
Highwood River	N/A (Stott, 1963, cross section 6-46 is faulted)	82J/9 849997 50°31′22.09″N 114°23′30.1″W	Walk
Kevin (Montana)	Cobban et al., 1976. Site 1A	48°47′36.3″N 111°56′27.83″W	Walk
	Site 1B	48°48′08.79″N 111°56′25.73″W	Walk
	Site 2	48°47′40.22″N 111°58′56.4″W	Walk
	Site 3A	48°49′04.54″N 111°59′50.66″W	Walk
	Site 3B	48°48′54.03″N 111°59′57.42″W	Walk
James River	Stott, 1963, cross section 6-5a	82O/14 291450 51°50′29.54″N 115°07′41.53W	Walk
Mill Creek	Wall, 1967, Wall and Rosene, 1977	82G/8 074728 49°22′28.2″N 114°08′40.94″W	Walk
Mill Ck – tributary	N/A	82G/8 075727 49°22′26.79″N 114°08′38.03″W	Walk
Lynx Creek	Stott, 1963, cross section 6-4	83B/4 769759 52°07′48.59″N 115°52′36.17″W	Walk
Oldfort Creek	N/A	82O/2 401674 51°08′26.86″N 114°59′50.8″W	Walk
Ram River	N/A	83B/4 795777 52°04′58.47″N 115°50′27.99″W	Walk
Sheep River	Stott, 1963, cross section 6-34	82J/10 654118 50°38′15.69″N 114°39′40.33″W	Walk
Sullivan Creek	N/A	82J/9 845007 50°31′54.56″N 114°23′46.9″W	Walk
Thistle Creek West	Stott, 1963, cross section 4-52	83C/15 095493 52°47′41.68″N 116°51′37.4″W	Walk
Thistle Creek East	N/A	83C/15 118497 52°47′53.48″N 116°49′32.1″W	Walk
Wapiabi Creek	Stott, 1963, cross section 4-6	83C/9 415263 52°35′19.39″N 116°23′18.29″W	Walk

APPENDIX 2

Results of Carbon Isotope Analyses of Samples from Cutpick Creek

Sample Number	TOC (wt %)	δ13C ‰ (VPDB)	Strat. Ht (m)
Cut 2 08-1	1.37	-26.26	0.2
Cut 2 08-2	1.09	-26.42	1.2
Cut 2 08-3	1.20	-26.37	2.2
Cut 2 08-4	1.13	-26.35	3.2
Cut 2 08-5	1.37	-26.38	4.2
Cut 2 08-6	1.38	-26.61	5.2
Cut 2 08-7	1.42	-26.51	6.2
Cut 2 08-8	1.39	-26.65	7.2
Cut 2 08-9	1.18	-26.74	8.2
Cut 2 08-10	1.31	-26.27	9.2
Cut 2 08-11	1.52	-26.10	10.2
Cut 2 08-12	1.27	-26.35	11.2
Cut 2 08-13	1.49	-26.21	12.2
Cut 2 08-14	1.38	-26.29	13.2
Cut 2 08-15	1.31	-26.08	14.2
Cut 2 08-16	1.21	-26.22	15.2
Cut 2 08-17	1.30	-26.17	16.2
Cut 2 08-18	0.87	-26.39	17.2
Cut 2 08-19	1.14	-26.48	18.2
Cut 2 08-20	1.37	-26.25	19.2
Cut 2 08-21	1.14	-26.53	20.2
Cut 2 08-22	1.24	-26.28	21.2
Cut 2 08-23	1.12	-26.30	22.2
Cut 2 08-24	1.12	-26.21	23.2
Cut 2 08-25	0.96	-26.42	24
Cut 2 08-26	1.14	-26.08	25.3
Cut 2 08-27	1.14	-25.84	26.6
Cut 2 08-28	0.83	-26.17	27.8
Cut 2 08-29	1.22	-25.95	29
Cut 2 08-30	0.97	-26.13	30.2
Cut 2 08-31	1.20	-26.07	31.2
Cut 2 08-32	1.06	-26.11	32.2
Cut 2 08-33	1.14	-26.05	33.2
Cut 2 08-34	1.21	-25.95	34.2
Cut 2 08-35	1.33	-25.62	35.2
Cut 2 08-36	1.33	-25.74	36.2

Sample Number	TOC (wt %)	δ13C ‰ (VPDB)	Strat. Ht (m)
Cut 2 08-37	0.99	-25.79	37.2
Cut 2 08-38	1.05	-25.92	38.2
Cut 2 08-39	1.14	-25.76	39.2
Cut 2 08-40	1.02	-25.80	40.2
Cut 2 08-41	1.09	-25.82	41.2
Cut 2 08-42	1.27	-25.76	42.1
Cut 2 08-43	1.22	-25.94	43.1
Cut 2 08-44	0.73	-26.33	44
Cut 2 08-45	1.06	-26.02	45
Cut 2 08-46	1.06	-25.86	46
Cut 2 08-47	1.14	-25.81	47
Cut 2 08-48	1.08	-25.83	48
Cut 2 08-49	1.17	-25.77	49
Cut 2 08-50	0.97	-25.84	50
Cut 2 08-51	1.04	-25.84	51
Cut 2 08-52	1.07	-25.88	52
Cut 2 08-53	1.04	-25.86	53
Cut 2 08-54	0.90	-25.81	54
Cut 2 08-55	1.06	-25.86	55
Cut 2 08-56	1.14	-25.71	56
Cut 2 08-57	0.97	-25.73	57
Cut 2 08-58	1.03	-25.82	58
Cut 2 08-59	1.13	-25.65	59
Cut 2 08-60	1.14	-25.65	60
Cut 2 08-61	1.22	-25.75	61
Cut 2 08-62	1.11	-25.59	62
Cut 2 08-63	1.21	-25.49	63
Cut 2 08-64	1.07	-25.56	64
Cut 2 08-65	1.05	-25.55	65
Cut 2 08-66	0.78	-25.77	66
Cut 2 08-67	1.17	-25.30	67
Cut 2 08-68	1.22	-25.33	68
Cut 2 08-69	1.06	-25.21	69
Cut 2 08-70	0.73	-26.06	70
Cut 2 08-71	1.20	-25.29	71.8
Cut 2 08-72	0.87	-25.78	72.8
Cut 2 08-73	0.62	-25.77	73.8
Cut 2 08-74	1.38	-25.29	74.8
Cut 2 08-75	0.94	-25.68	75.8

Sample Number	TOC (wt %)	δ13C ‰ (VPDB)	Strat. Ht (m)
Cut 2 08-76	0.94	-25.51	76.8
Cut 2 08-77	0.80	-25.71	77.8
Cut 2 08-78	1.01	-25.30	78.8
Cut 2 08-79	1.16	-25.31	79.5
Cut 2 08-80	0.71	-25.50	80.5
Cut 2 08-81	0.54	-25.53	81.7
Cut 2 08-82	0.78	-25.28	82.9
Cut 2 08-83	0.73	-25.37	83.9
Cut 2 08-84	0.72	-25.43	85
Cut 2 08-85	0.89	-25.31	85.9
Cut 2 08-86	1.20	-25.47	86.2
Cut 2 08-87	1.34	-25.27	87.5
Cut 2 08-88	1.15	-25.58	88.3
Cut 2 08-89	0.87	-25.62	89.3
Cut 2 08-90	0.77	-25.71	90.3
Cut 2 08-91	1.05	-25.72	91.3
Cut 2 08-92	1.16	-25.47	92.4
Cut 2 08-93	0.76	-25.80	93.4
Cut 2 08-94	0.65	-25.74	94.4
Cut 2 08-95	1.04	-25.48	95.4
Cut 2 08-96	1.57	-25.14	96.4
Cut 2 08-97	2.52	-24.19	98.2
Cut 2 08-98	1.10	-25.16	100.3
Cut 2 08-99	0.39	-26.44	102.3
Cut 2 08-100	0.88	-25.37	104.2
Cut 2 08-101	0.76	-25.11	105.3
Cut 2 08-102	1.42	-25.10	106.8
Cut 2 08-103	1.35	-24.82	107.8
Cut 2 08-104	1.35	-25.05	108.8
Cut 2 08-105	1.35	-24.86	110.5
Cut 2 08-106	2.51	-24.71	111.3
Cut 2 08-107	1.20	-26.24	113.5
Cut 2 08-108	1.19	-25.89	114.5

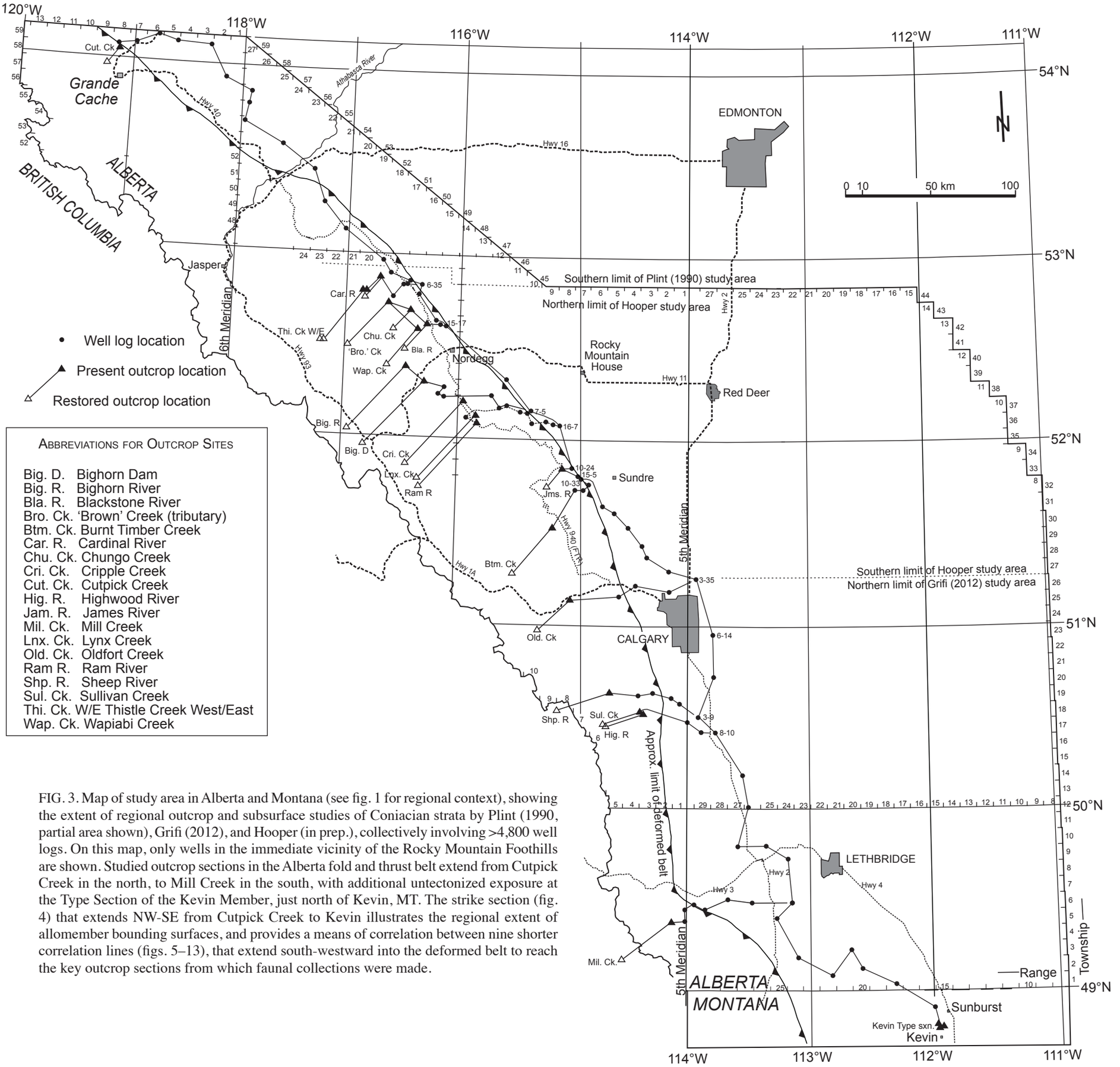

Abbreviations for Outcrop Sites

Big. D. Bighorn Dam
Big. R. Bighorn River
Bla. R. Blackstone River
Bro. Ck. 'Brown' Creek (tributary)
Btm. Ck. Burnt Timber Creek
Car. R. Cardinal River
Chu. Ck. Chungo Creek
Cri. Ck. Cripple Creek
Cut. Ck. Cutpick Creek
Hig. R. Highwood River
Jam. R. James River
Mil. Ck. Mill Creek
Lnx. Ck. Lynx Creek
Old. Ck. Oldfort Creek
Ram R. Ram River
Shp. R. Sheep River
Sul. Ck. Sullivan Creek
Thi. Ck. W/E Thistle Creek West/East
Wap. Ck. Wapiabi Creek

FIG. 3. Map of study area in Alberta and Montana (see fig. 1 for regional context), showing the extent of regional outcrop and subsurface studies of Coniacian strata by Plint (1990, partial area shown), Grifi (2012), and Hooper (in prep.), collectively involving >4,800 well logs. On this map, only wells in the immediate vicinity of the Rocky Mountain Foothills are shown. Studied outcrop sections in the Alberta fold and thrust belt extend from Cutpick Creek in the north, to Mill Creek in the south, with additional untectonized exposure at the Type Section of the Kevin Member, just north of Kevin, MT. The strike section (fig. 4) that extends NW-SE from Cutpick Creek to Kevin illustrates the regional extent of allomember bounding surfaces, and provides a means of correlation between nine shorter correlation lines (figs. 5–13), that extend south-westward into the deformed belt to reach the key outcrop sections from which faunal collections were made.

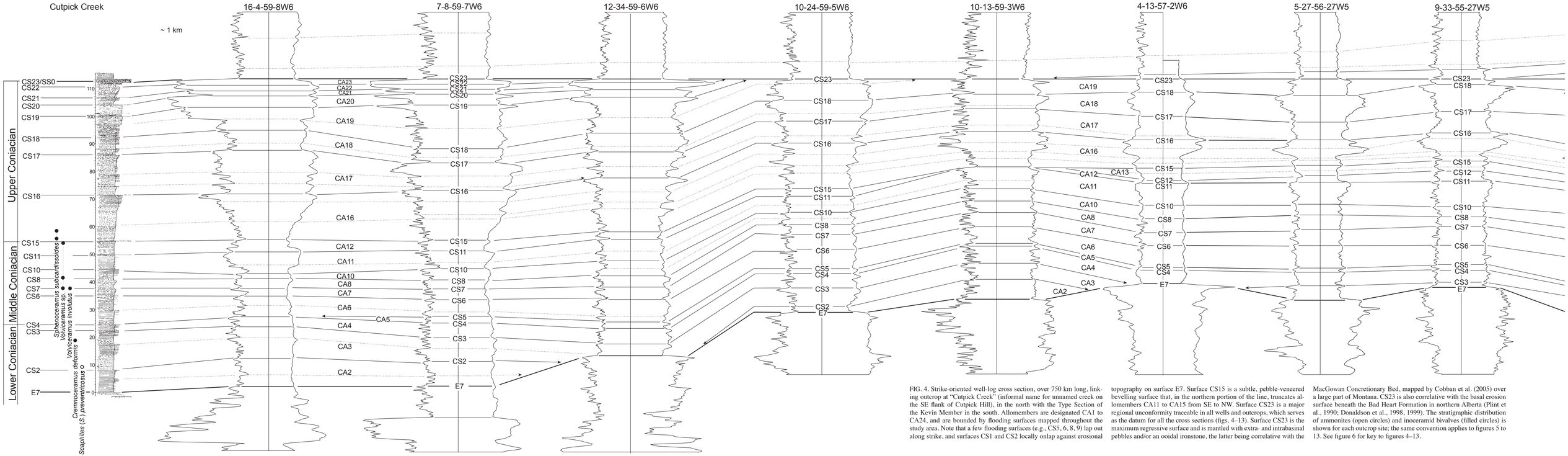

FIG. 4. Strike-oriented well-log cross section, over 750 km long, linking outcrop at "Cutpick Creek" (informal name for unnamed creek on the SE flank of Cutpick Hill), in the north with the Type Section of the Kevin Member in the south. Allomembers are designated CA1 to CA24, and are bounded by flooding surfaces mapped throughout the study area. Note that a few flooding surfaces (e.g., CS5, 6, 8, 9) lap out along strike, and surfaces CS1 and CS2 locally onlap against erosional topography on surface E7. Surface CS15 is a subtle, pebble-veneered bevelling surface that, in the northern portion of the line, truncates allomembers CA11 to CA15 from SE to NW. Surface CS23 is a major regional unconformity traceable in all wells and outcrops, which serves as the datum for all the cross sections (figs. 4–13). Surface CS23 is the maximum regressive surface and is mantled with extra- and intrabasinal pebbles and/or an ooidal ironstone, the latter being correlative with the MacGowan Concretionary Bed, mapped by Cobban et al. (2005) over a large part of Montana. CS23 is also correlative with the basal erosion surface beneath the Bad Heart Formation in northern Alberta (Plint et al., 1990; Donaldson et al., 1998, 1999). The stratigraphic distribution of ammonites (open circles) and inoceramid bivalves (filled circles) is shown for each outcrop site; the same convention applies to figures 5 to 13. See figure 6 for key to figures 4–13.

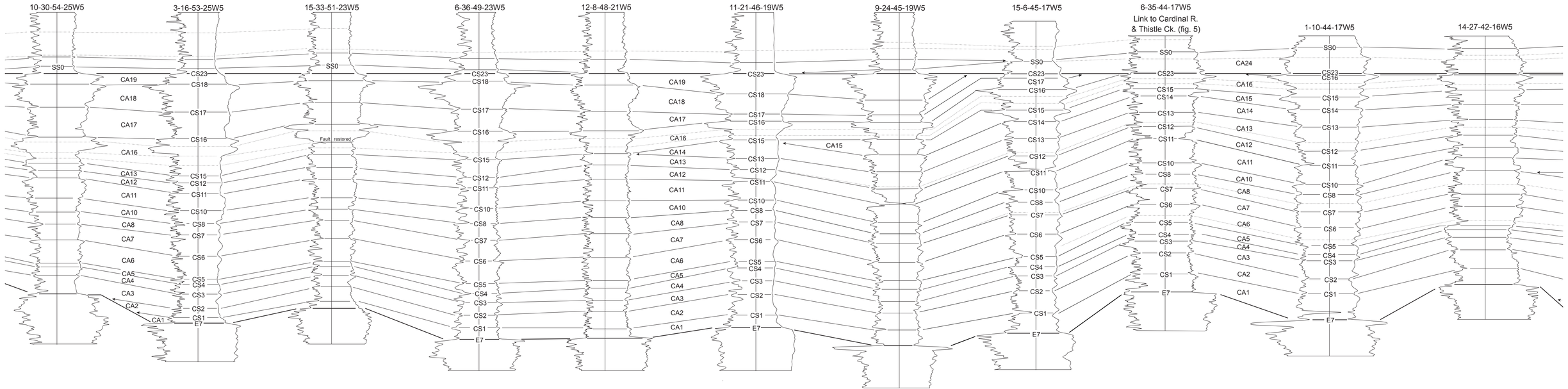
10-30-54-25W5
3-16-53-25W5
15-33-51-23W5
6-36-49-23W5
12-8-48-21W5
11-21-46-19W5
9-24-45-19W5
15-6-45-17W5
6-35-44-17W5
Link to Cardinal R.
& Thistle Ck. (fig. 5)
1-10-44-17W5
14-27-42-16W5
Fault restored
SS0
CS23
CS18
CS17
CS16
CS15
CS12
CS11
CS10
CS8
CS7
CS6
CS5
CS4
CS3
CS2
CS1
E7
CA19
CA18
CA17
CA16
CA15
CA14
CA13
CA12
CA11
CA10
CA8
CA7
CA6
CA5
CA4
CA3
CA2
CA1
CS17
CS14
CS13
CA24

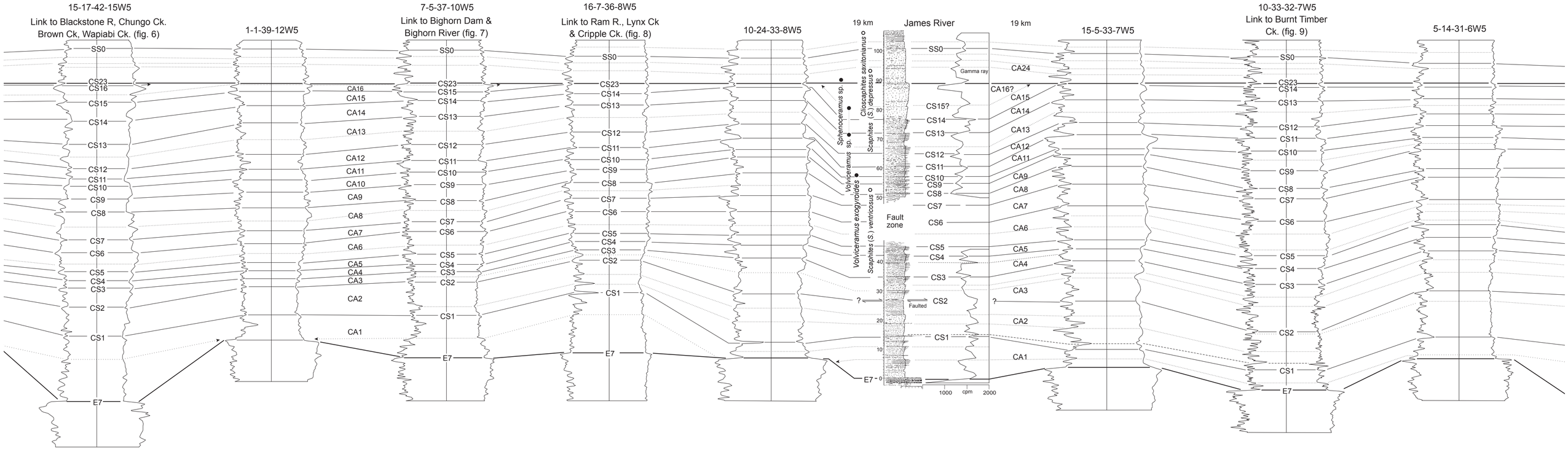
15-17-42-15W5
Link to Blackstone R, Chungo Ck.
Brown Ck, Wapiabi Ck. (fig. 6)
1-1-39-12W5
7-5-37-10W5
Link to Bighorn Dam &
Bighorn River (fig. 7)
16-7-36-8W5
Link to Ram R., Lynx Ck
& Cripple Ck. (fig. 8)
10-24-33-8W5
19 km
James River
19 km
15-5-33-7W5
10-33-32-7W5
Link to Burnt Timber
Ck. (fig. 9)
5-14-31-6W5
Closcaphites saxitonianus
Sphenoceramus sp.
Scaphites (S.) depressus
Volviceramus sp.
Volviceramus exogyroides
Scaphites (S.) ventricosus
Fault
zone
Faulted
Gamma ray
1000
cpm
2000
SS0
CS23
CS16
CS15
CS14
CS13
CS12
CS11
CS10
CS9
CS8
CS7
CS6
CS5
CS4
CS3
CS2
CS1
E7
CA16
CA15
CA14
CA13
CA12
CA11
CA10
CA9
CA8
CA7
CA6
CA5
CA4
CA3
CA2
CA1
CA24
CA16?
CS15?

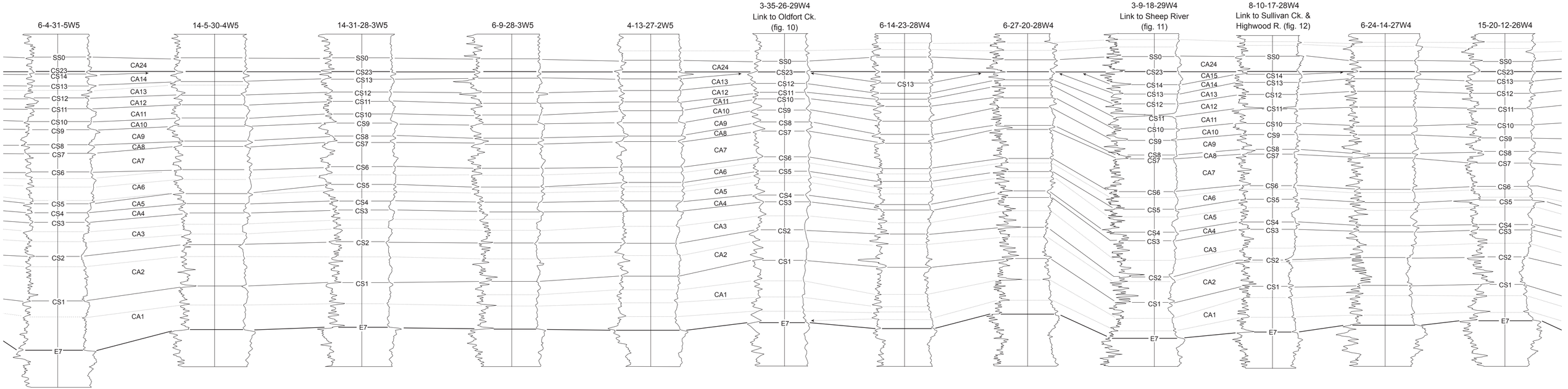
6-4-31-5W5
14-5-30-4W5
14-31-28-3W5
6-9-28-3W5
4-13-27-2W5
3-35-26-29W4
Link to Oldfort Ck.
(fig. 10)
6-14-23-28W4
6-27-20-28W4
3-9-18-29W4
Link to Sheep River
(fig. 11)
8-10-17-28W4
Link to Sullivan Ck. &
Highwood R. (fig. 12)
6-24-14-27W4
15-20-12-26W4
SS0
CS23
CS14
CS13
CS12
CS11
CS10
CS9
CS8
CS7
CS6
CS5
CS4
CS3
CS2
CS1
E7
CA24
CA14
CA13
CA12
CA11
CA10
CA9
CA8
CA7
CA6
CA5
CA4
CA3
CA2
CA1
CA15

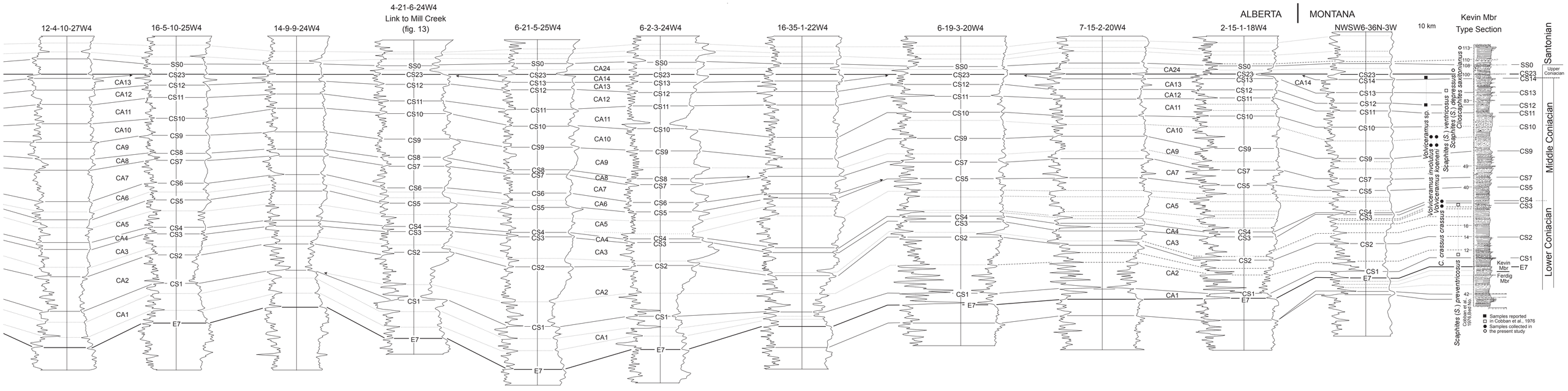
12-4-10-27W4
16-5-10-25W4
14-9-9-24W4
4-21-6-24W4
Link to Mill Creek
(fig. 13)
6-21-5-25W4
6-2-3-24W4
16-35-1-22W4
6-19-3-20W4
7-15-2-20W4
2-15-1-18W4
NWSW6-36N-3W
ALBERTA
MONTANA
10 km
Kevin Mbr
Type Section
Santonian
Upper Coniacian
Middle Coniacian
Lower Coniacian
Kevin Mbr
Ferdig Mbr
E7
Volviceramus sp.
Volviceramus involutus
Volviceramus koeneni
Scaphites (S.) ventricosus
Clioscaphites saxitonianus
C. crassus crassus
Scaphites (S.) preventricosus
Cobban et al., 1976 type locality
Samples reported in Cobban et al., 1976
Samples collected in the present study

FIG. 5. Correlation of outcrop sections on Thistle Creek and Cardinal River with the regional allostratigraphic framework. Principal correlation points are provided by the major transgressive event at E7, a major flooding surface at CS4, an abrupt change from weak to intense bioturbation at CS14, and a maximum regressive surface at CS23.

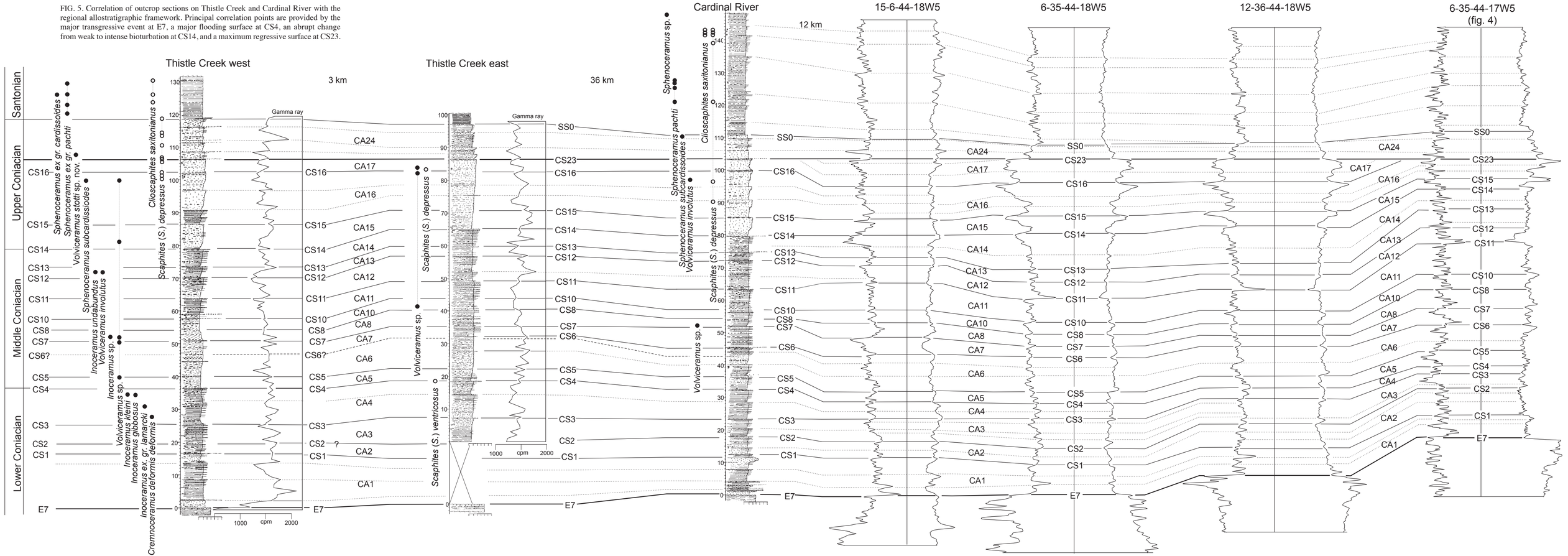

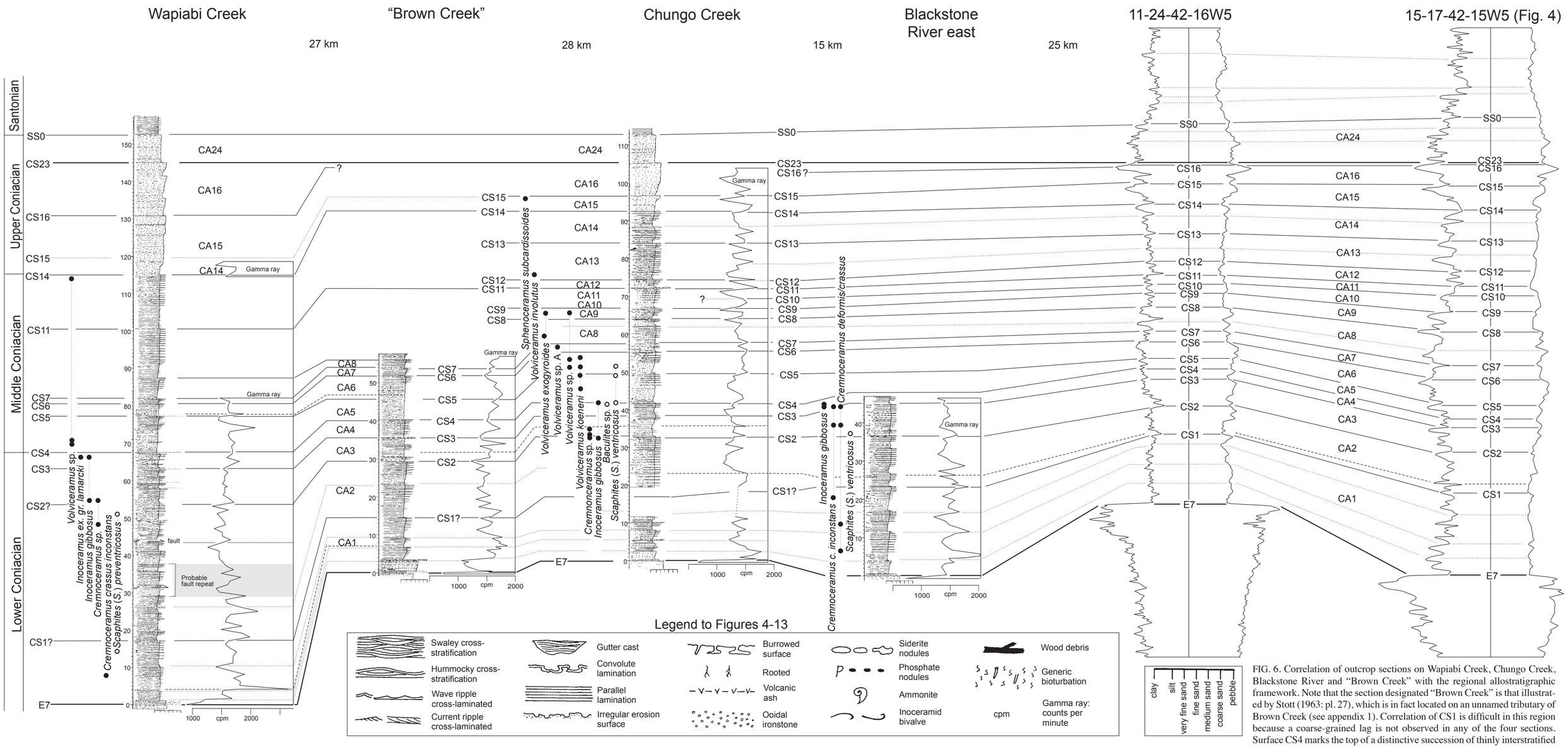

FIG. 6. Correlation of outcrop sections on Wapiabi Creek, Chungo Creek, Blackstone River and "Brown Creek" with the regional allostratigraphic framework. Note that the section designated "Brown Creek" is that illustrated by Stott (1963: pl. 27), which is in fact located on an unnamed tributary of Brown Creek (see appendix 1). Correlation of CS1 is difficult in this region because a coarse-grained lag is not observed in any of the four sections. Surface CS4 marks the top of a distinctive succession of thinly interstratified sandstone and mudstone; CS14 and CS23 are also easily recognized.

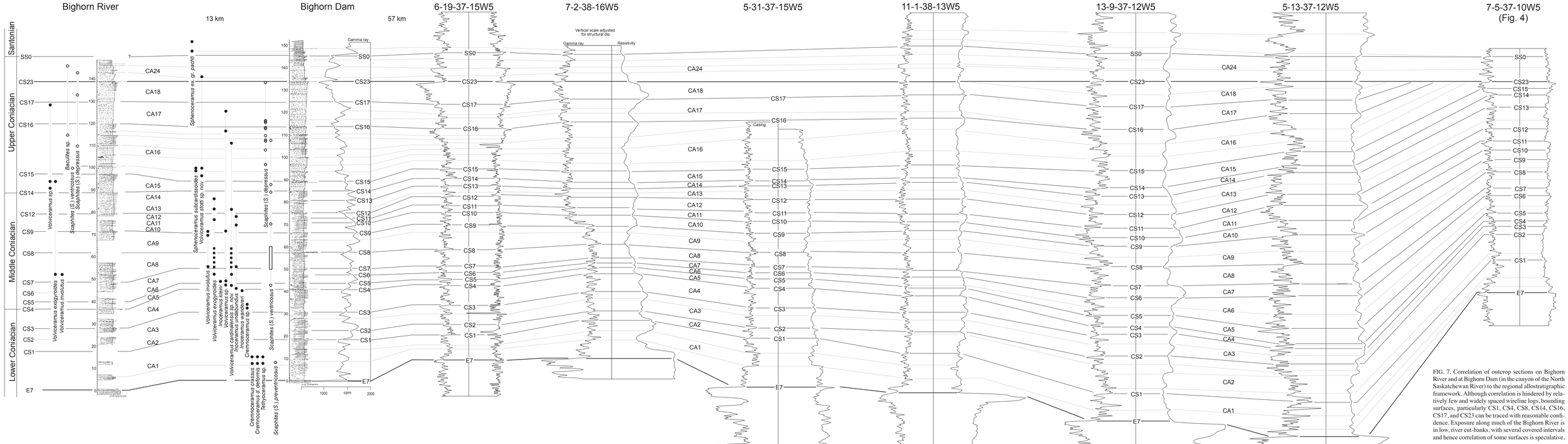

FIG. 7. Correlation of outcrop sections on Bighorn River and at Bighorn Dam (in the canyon of the North Saskatchewan River) to the regional allostratigraphic framework. Although correlation is hindered by relatively few and widely spaced wireline logs, bounding surfaces, particularly CS1, CS4, CS8, CS14, CS16, CS17, and CS23 can be traced with reasonable confidence. Exposure along much of the Bighorn River is in low, river cut-banks, with several covered intervals and hence correlation of some surfaces is speculative.

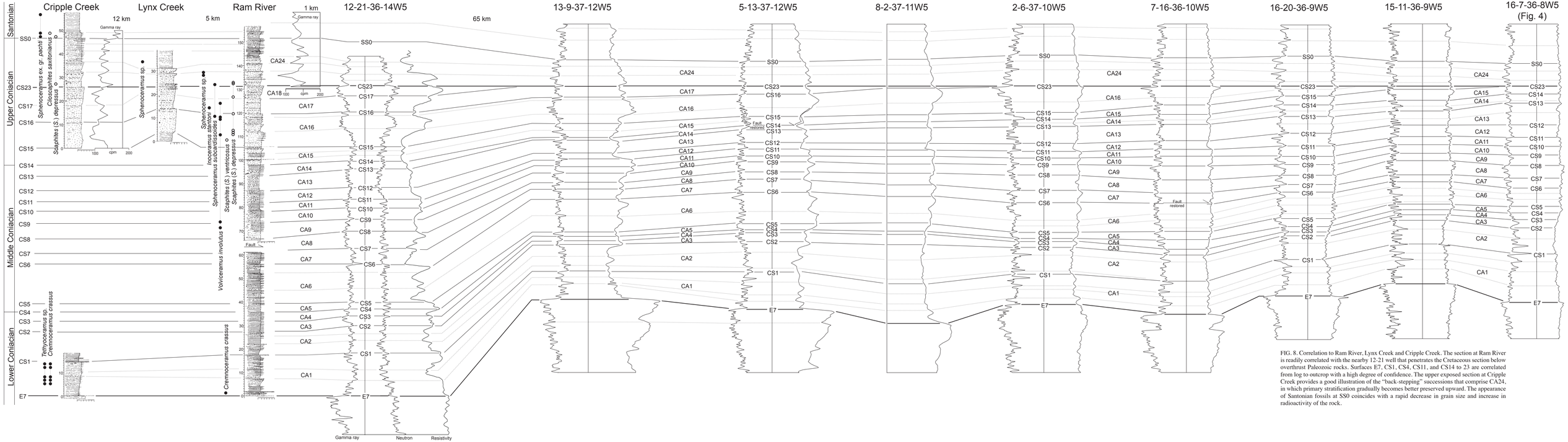

FIG. 8. Correlation to Ram River, Lynx Creek and Cripple Creek. The section at Ram River is readily correlated with the nearby 12-21 well that penetrates the Cretaceous section below overthrust Paleozoic rocks. Surfaces E7, CS1, CS4, CS11, and CS14 to 23 are correlated from log to outcrop with a high degree of confidence. The upper exposed section at Cripple Creek provides a good illustration of the "back-stepping" successions that comprise CA24, in which primary stratification gradually becomes better preserved upward. The appearance of Santonian fossils at SS0 coincides with a rapid decrease in grain size and increase in radioactivity of the rock.

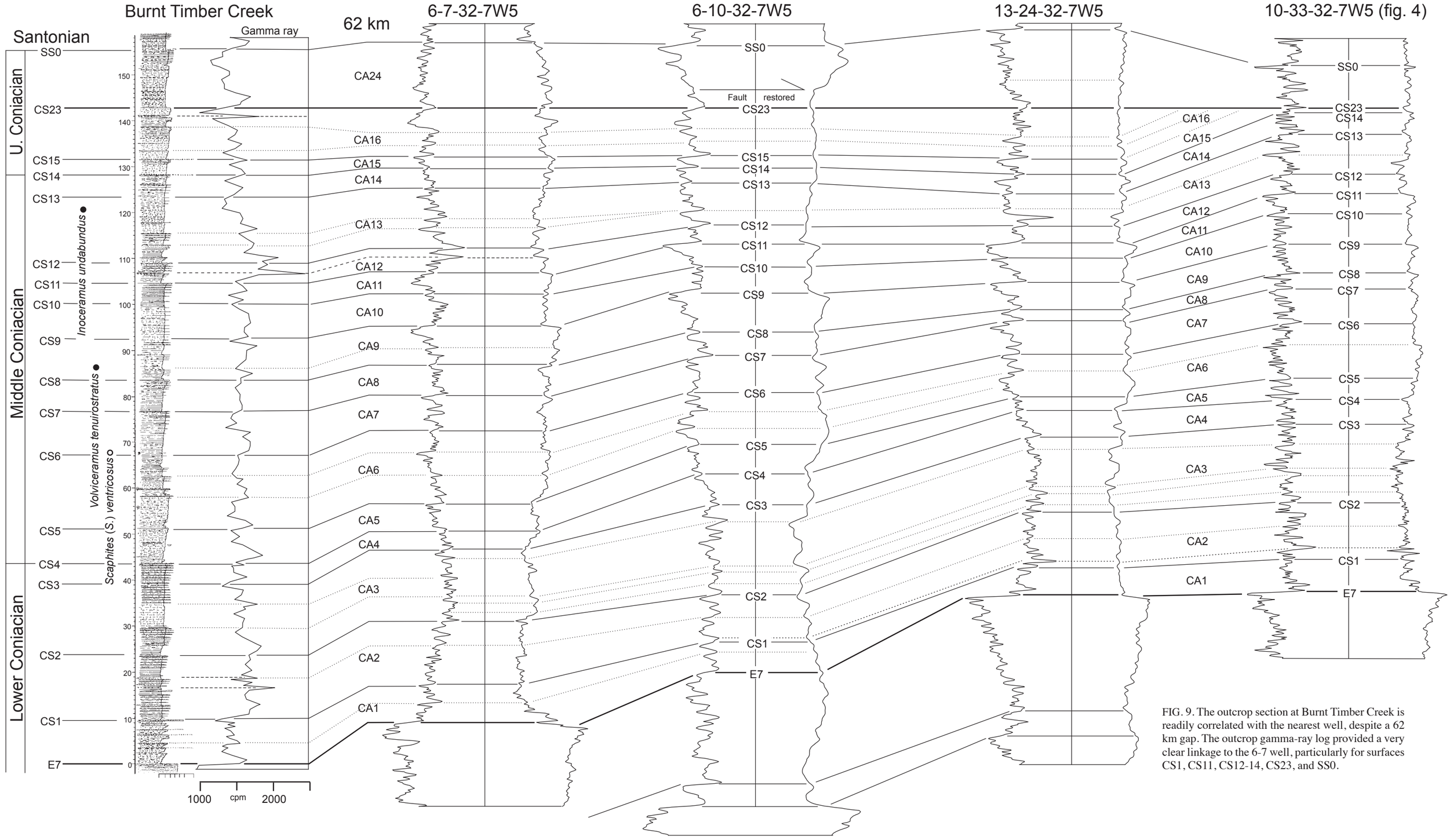

FIG. 9. The outcrop section at Burnt Timber Creek is readily correlated with the nearest well, despite a 62 km gap. The outcrop gamma-ray log provided a very clear linkage to the 6-7 well, particularly for surfaces CS1, CS11, CS12-14, CS23, and SS0.

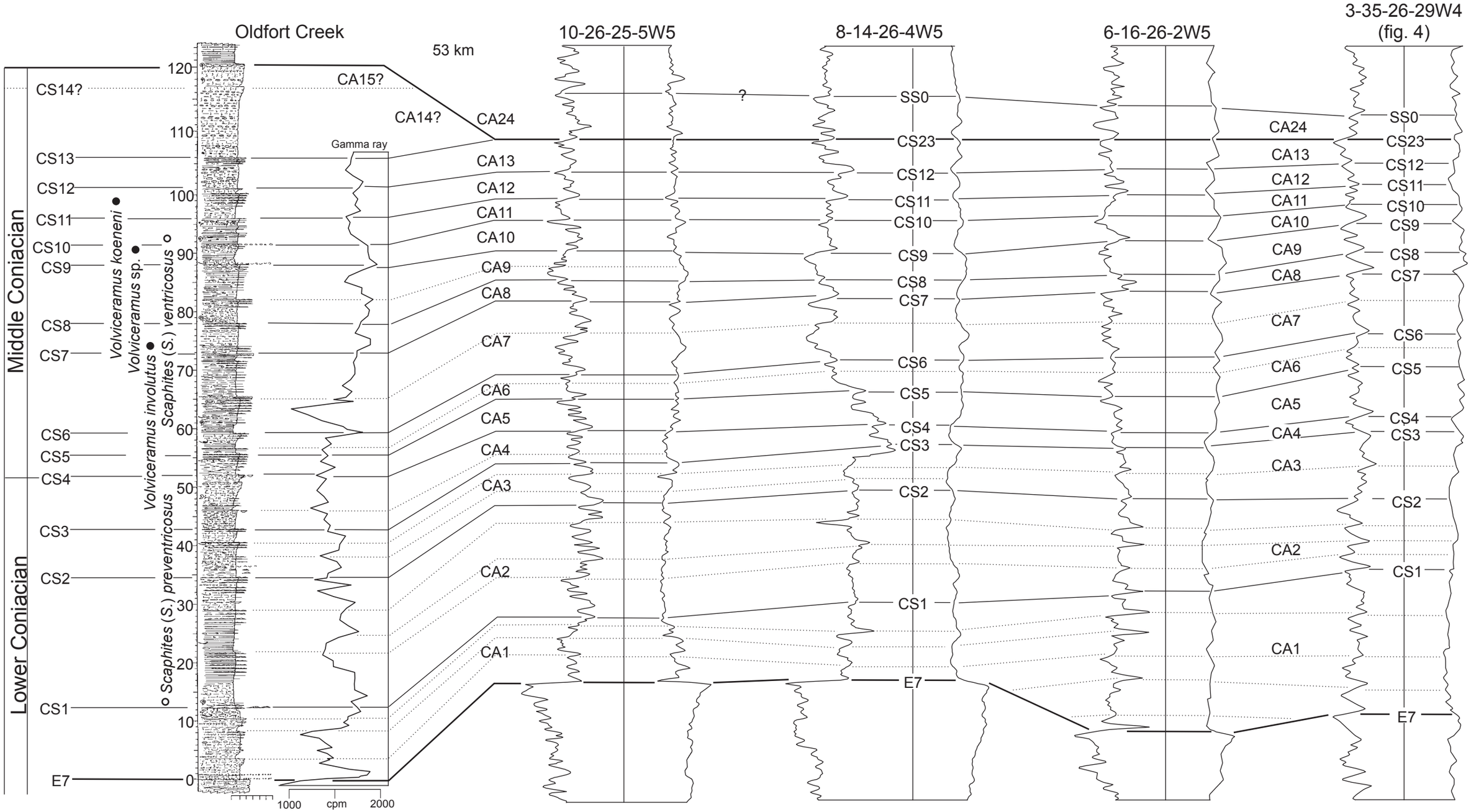

FIG. 10. The section at Oldfort Creek is compiled from several separate, but overlapping sections exposed in Oldfort Creek and beside the Bow River. The outcrop gamma-ray log helps to establish tie-points, such as CS1, CS6, CS7, and CS11.

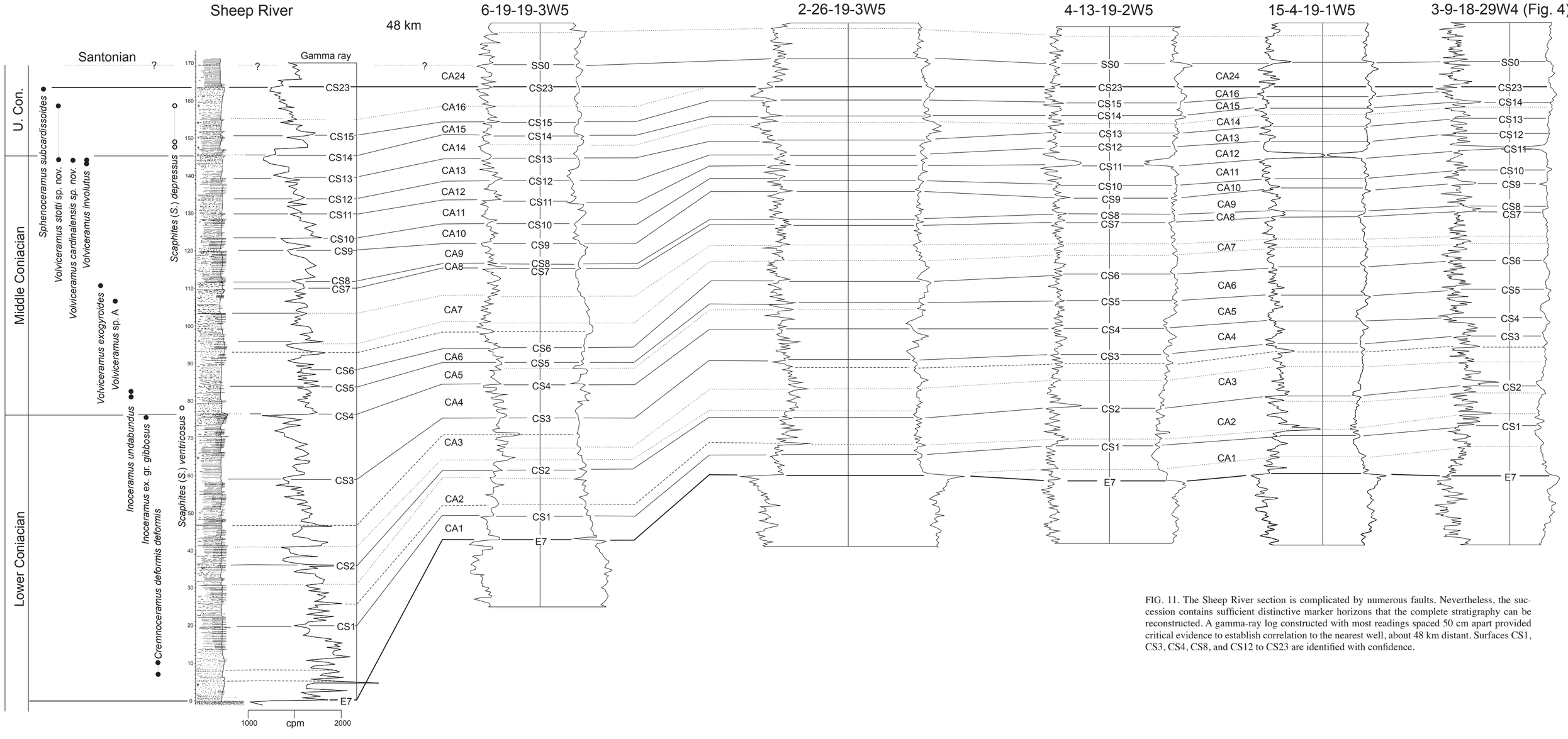

FIG. 11. The Sheep River section is complicated by numerous faults. Nevertheless, the succession contains sufficient distinctive marker horizons that the complete stratigraphy can be reconstructed. A gamma-ray log constructed with most readings spaced 50 cm apart provided critical evidence to establish correlation to the nearest well, about 48 km distant. Surfaces CS1, CS3, CS4, CS8, and CS12 to CS23 are identified with confidence.

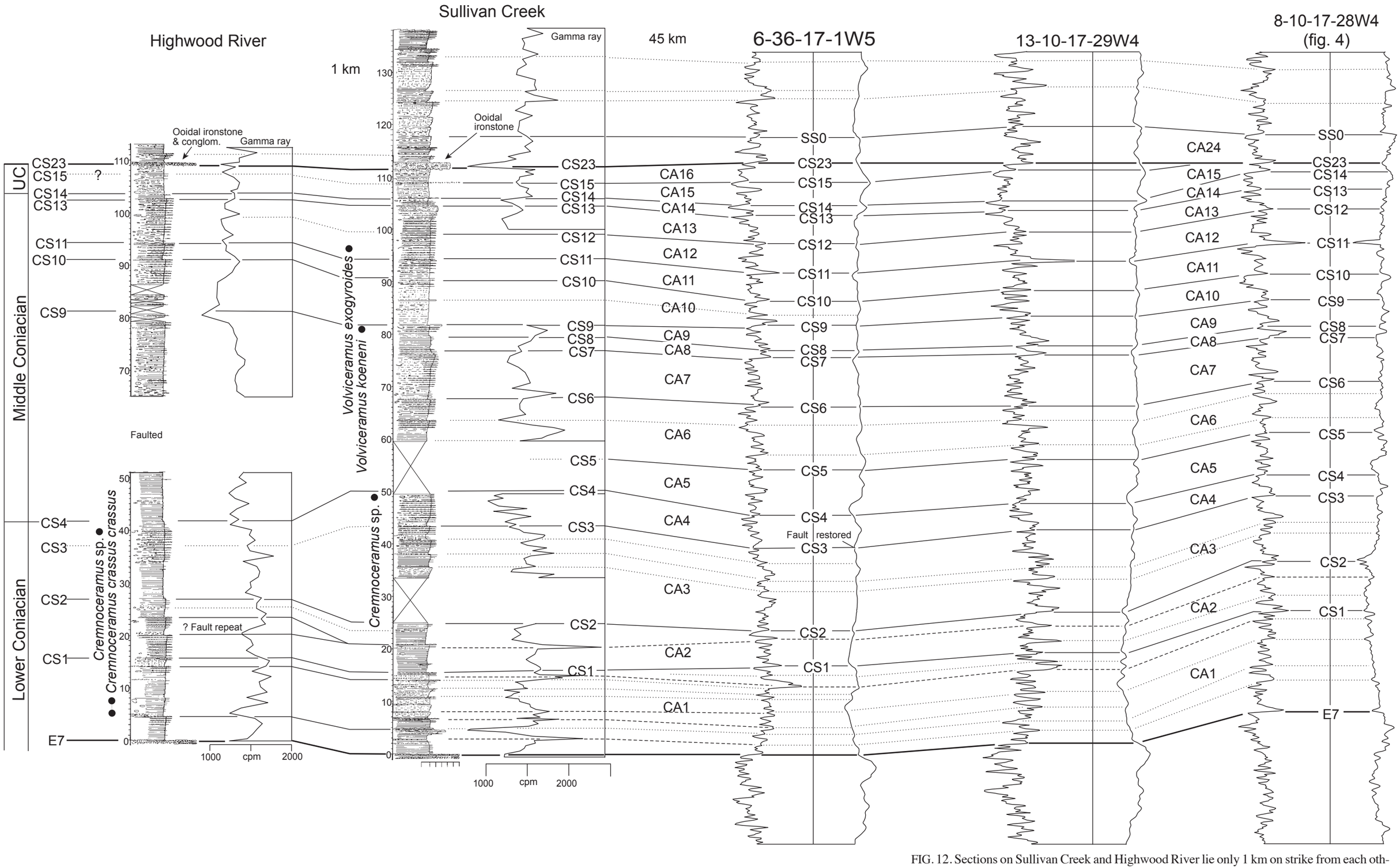

FIG. 12. Sections on Sullivan Creek and Highwood River lie only 1 km on strike from each other on the same thrust slice. Surface CS1 seems to lack a coarse-grained lag; surfaces CS4, CS7, CS14, CS15, and CS23 are identified with confidence. At Sullivan Creek, a 1.2 m thick ooidal ironstone containing scattered small chert pebbles lies immediately above CS23 (fig. 17A); the basal surface of the ironstone is penetrated by abundant large arthropod burrows (fig. 17B),

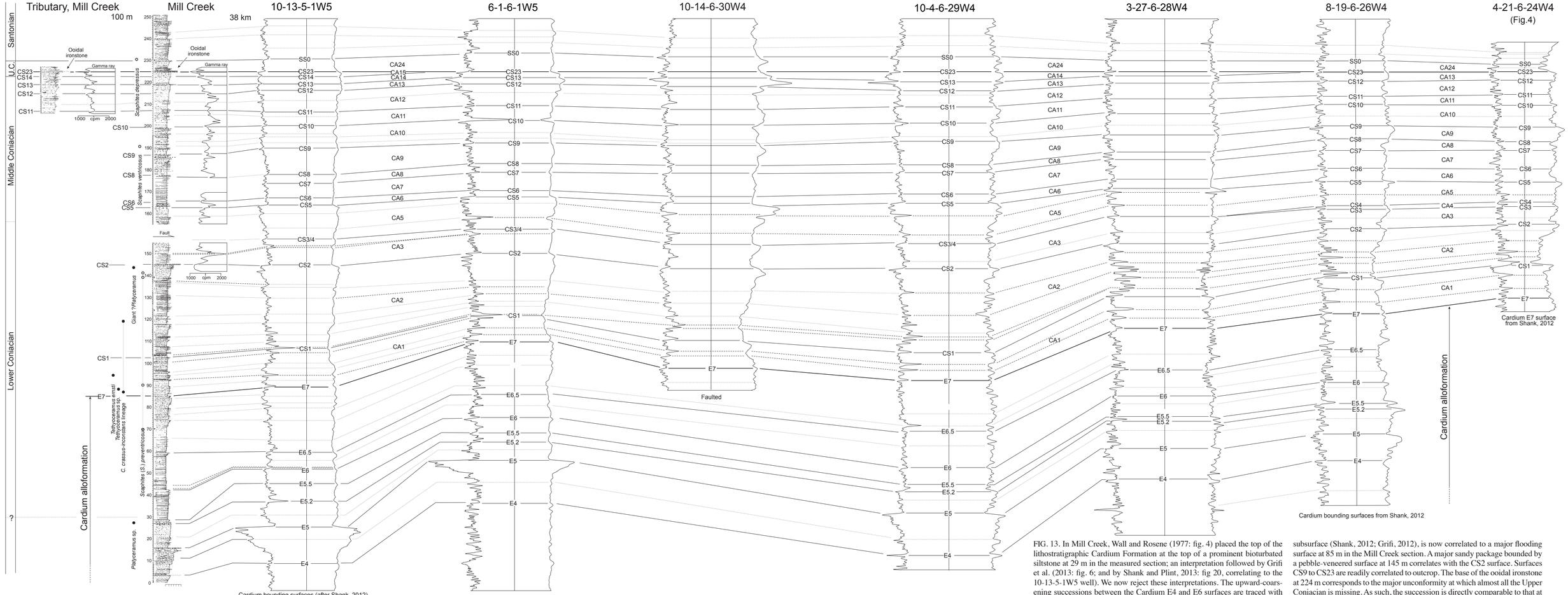

FIG. 13. In Mill Creek, Wall and Rosene (1977: fig. 4) placed the top of the lithostratigraphic Cardium Formation at the top of a prominent bioturbated siltstone at 29 m in the measured section; an interpretation followed by Grifi et al. (2013: fig. 6; and by Shank and Plint, 2013: fig 20, correlating to the 10-13-5-1W5 well). We now reject these interpretations. The upward-coarsening successions between the Cardium E4 and E6 surfaces are traced with confidence from log to outcrop. The E7 unconformity, widely mapped in subsurface (Shank, 2012; Grifi, 2012), is now correlated to a major flooding surface at 85 m in the Mill Creek section. A major sandy package bounded by a pebble-veneered surface at 145 m correlates with the CS2 surface. Surfaces CS9 to CS23 are readily correlated to outcrop. The base of the ooidal ironstone at 224 m corresponds to the major unconformity at which almost all the Upper Coniacian is missing. As such, the succession is directly comparable to that at Highwood River, Sullivan Creek and Kevin.